Inflammation and intervertebral disc degeneration in dogs

Research Project Veterinary Medicine University Utrecht

Saskia van Dongen, 3577139

Supervisor: drs. Nicole Willems

03/02/2014 – 31/04/2014

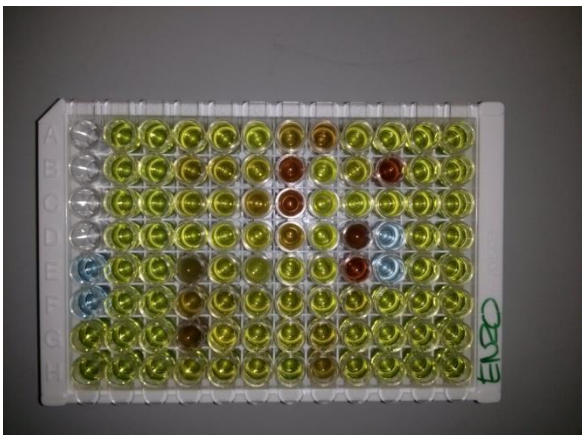

Prefactory note

Within the training of Veterinary Medicine at the University of Utrecht all students have to fulfill a research project. This paper is the final report of the research project performed by Saskia van Dongen as research student at the Orthopedic research team. This study was performed to investigate whether the PGE2 levels in IVDs of dogs suffering from chronic low back pain, are correlated with higher grades of disc degeneration.

Table of contents

Summary

Intervertebral disc (IVD) degeneration is an abnormal, cell-mediated response to progressive structural failure of the IVD. IVD degeneration is more common in chondrodystrophic (CD) dogs than in non-chondrodystrophic (NCD) dogs. In CD dogs IVD degeneration progresses quickly and results in Hansen type I herniation. In NCD dogs degeneration has a gradual character and results in Hansen type II herniation. The Pfirrmann grading system is used to grade IVD degeneration on the basis of magnetic resonance imaging (MRI) findings.
The goal of this research is to investigate whether the PGE2 levels in IVDs of dogs suffering from chronic low back pain, are correlated with higher grades of disc degeneration.
IVD tissue was collected from canine patients that underwent surgery at the University Clinic for Companion Animals in Utrecht. All the sample IVDs were graded by using the Pfirmann grading system and afterwards the samples were classified in groups on the basis of their Pfirrmann score, NCD/CD classification and the fact whether herniation occurred or not. The PGE2 content, DNA content, protein content and GAG content of the samples were measured. To examine COX-2 protein expression on histological samples, a COX-2 immunohistochemical staining was performed.
A difference was found between PGE2/weight ratios and PGE2/DNA ratios, which can be explained by the cellularity of the samples. In this study the weight of the samples appeared to be a better correction factor for the PGE2 content. The PGE2/protein content ratio was not a reliable measure to represent PGE2 contents. The PGE2 content in the NP appeared to be higher than in the AF. Furthermore, our results suggest that the lack of clinical signs is associated with a lower PGE2 content. Our results support findings in literature that the GAG/weight ratio in the NP is negatively correlated with increasing degeneration. A decrease in GAG content was seen in the NP as degeneration increases. We did not find an increase in GAG content in the AF as degeneration increased.
Our dataset turned out to be too small to test whether there is a correlation between PGE2 levels and Pfirrmann score. The COX-2 immunohistochemical staining appeared to be not specific enough and needs further optimization before patient samples can be tested.

Introduction

The healthy canine intervertebral disc

The healthy IVD consists of four distinct components, namely, the nucleus pulposus (NP), annulus fibrusos (AF), endplates (EP) and transitional zone (TZ) (Figure 1)(N. Bergknut, Smolders et al., 2013; Cappello, Bird, Pfeiffer, Bayliss, & Dudhia, 2006; Johnson, Da Costa, & Allen, 2010).

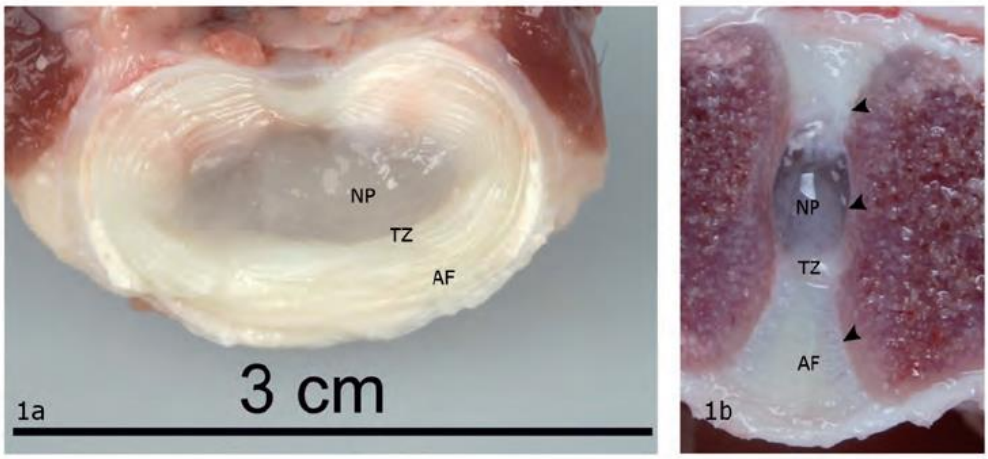

Figure 1: Transverse (a) and sagittal (b) section through a L5-L6 intervertebral disc of a mature non-chondrodystrophic dog, showing the nucleus pulposus (NP), transition zone (TZ), annulus fibrosus (AF), and endplates (EP)(P. N. Bergknut, 2011).

- Nucleus pulposus

The NP (nucleus pulposus) is a mucous, transparent and bean-shaped structure in the centre of the IVD. The healthy NP is composed of a complex network of negatively charged proteoglycans interwoven in a network of collagen fibers. The proteoglycan molecules consist of a protein backbone with negatively charged glycosaminoglycan side chains (GAGs). The most common side chains are chondroitin sulfate and keratin sulfate. The proteoglycans are in turn aggregated with hyaluronic acid. In this way, negatively charged large complexes are formed that create a strong osmotic gradient, attracting water into the NP. As a result, over 80% of the healthy NP is composed of water, leading to a high intradiscal pressure. In healthy, non-degenerated IVDs, notochordal cells (NCs) are present in the NP. Notochordal cells are thought to secrete factors that protect the NP cells from degradation and apoptosis(Erwin, Islam, Inman, Fehlings, & Tsui, 2011). Furthermore, the NP is an avascular structure(N. Bergknut et al., 2013; Urban, Smith, & Fairbank, 2004).

- Annulus Fibrosus en Transition Zone

The NP is surrounded by the AF (annulus fibrosus). This is a dense network of multiple, organized, concentric fibrous lamellae. Closer to the centre of the IVD, the AF becomes more cartilaginous and less fibrous. This region is called the transition zone (TZ) , and forms the interconnection between the NP and AF(N. Bergknut et al., 2013).

- Endplates

The cranial and caudal borders of the IVD are formed by the cartilaginous endplates (EPs). The EPs are necessary for supplying the IVD with nutrients. Small molecules reach the cells of the NP, TZ, and AF through diffusion and osmosis, larger molecules are transported by a

pumping mechanism created by the physiological loading of the IVD (Adams & Roughley, 2006; Roberts, McCall, Menage, Haddaway, & Eisenstein, 1997; Urban et al., 2004).

The degenerating canine intervertebral disc

IVD degeneration is as an abnormal, cell-mediated response to progressive structural failure of the IVD. IVD degeneration can be seen as a multifactorial process. A genetic predisposition exists, and other factors leading to IVD degeneration can be mechanical overload and trauma, inadequate metabolite and nutrient transport to and from the cells within the IVD matrix, altered levels of enzyme activity, changes in matrix macromolecules and changes in water content. In the process of IVD degeneration, the GAG content and collagen type II in the NP decrease. At the same time, the collagen type I content increases. As a result, the matrix of the IVD becomes more rigid. This leads to impairment of its biomechanical function. Because of the structural failure, the biomechanical environment of the IVD cells changes and causes impairment of the diffusion of nutrients. This leads to further deterioration of the IVD cells. Furthermore, the IVD cells are not able to adequately repair the matrix. The IVD weakens and gets vulnerable to physiological levels of stress. This process can be seen as a vicious cycle of continued damage and inadequate repair, resulting in degeneration of the IVD. Characteristic macroscopic changes can be found, such as a decreasing disc height due to dehydration of the IVD (Figure 2). In the degenerating EP, the water, collagen type II and proteoglycan content decreases and mineralization of the EPs may occur. Capillaries may become obstructed because of degeneration of the EP and sclerosis of the subchondral bone. This will lead to a disturbed transport of solutes to and from the IVD. Because of the decreased functionality of the NP, the AF and EPs are loaded non-physiologically and this may result in annular tears and EP fractures. Structural failure of the IVD as a whole may result in bulging or herniation of the IVD (Adams & Roughley, 2006; N. Bergknut et al., 2013).

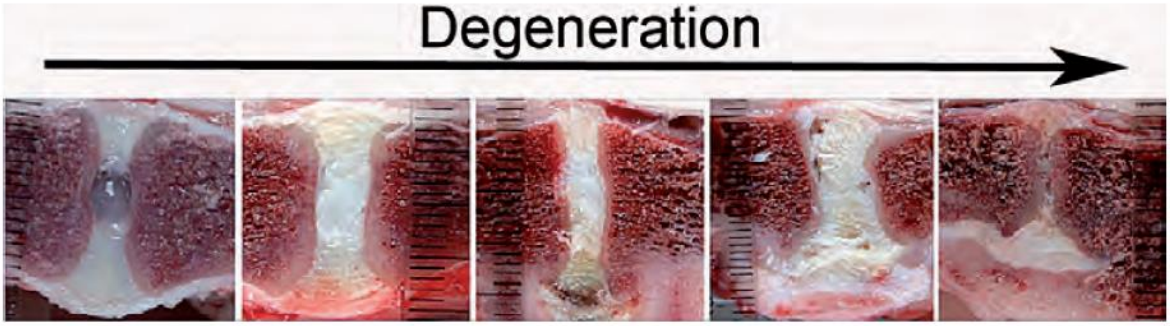

Figure 2: Sagittal sections through intervertebral discs. Different stages of degeneration can be seen by macroscopic changes in the nucleus pulposus, annulus fibrosus, endplates and vertebral bodies. From the left to the right the degeneration increases(Hazewinkel, Meij, Bergknut, Tryfonidou, & Smolders, 2013).

Chondrodystrophic and non-chondrodystrophic breeds

Intervertebral disc (IVD) degeneration can occur in all types of dog breeds. Dog breeds can be classified into two groups, based on the predisposition to chondrodystrophy; chondrodystrophic (CD) and non-chondrodystrophic (NCD). Next to the different process of endochondral ossification in both type of dogs, differences exist with regard to the age of onset, frequency, and spinal location of IVD degeneration and IVD degenerative diseases(Smolders et al., 2013).

Chondrodystrophic dogs

CD dogs have a disturbed endochondral ossification in the growth plates. The growth plates calcify earlier than usual resulting in shortened bones. Especially the long bones are affected and they have a curved appearance (P. N. Bergknut, 2011; Parker et al., 2009; Smolders et al., 2013). Some popular CD breeds are the (miniature) Dachshund, Basset Hound, French and English Bulldog, Shi Tzu, miniature Schnauzer, Pekingese, Beagle, Lhasa Apso, Bichon Frisé, Tibetan Spaniel, Cavalier King Charles Spaniel, Welsh Corgi, and the American Cocker Spaniel. IVD degeneration is more common in CD dogs than in NCD dogs. In CD dogs, IVD degenerative disease usually develops around 3–7 years of age and mostly affects the cervical or thoracolumbar spine (Brisson, 2010; Parker et al., 2009).

Figure 3: Examples of CD and NCD breeds (Left side: Pembroke Welsh corgi, basset hound, and dachshund (CD), right side: collie, whippet, and German shepherd dog (NCD)(Parker et al., 2009).

CD dogs develop IVD degeneration at an earlier age than NCD dogs and the degeneration progresses more rapidly. In CD dogs, the change from a jellylike NP to a dehydrated NP can already be seen at 3–4 months of age. At one year of age, the majority of the IVDs have undergone this transformation and in the end they will all be affected(P. N. Bergknut, 2011; Smolders et al., 2013).

Furthermore, the NP of CD dogs is progressively substituted by chondrocyte-like cells, surrounded by a comprehensive and dense extracellular matrix. This process of chondrification spreads throughout the NP until at approximately one year of age the whole NP has undergone this so-called chondroid metamorphosis. Chondrocyte-like cells frequently go in apoptosis(P. N. Bergknut, 2011; Smolders et al., 2013).

According to Hansen (1952), AF degeneration will not develop autonomously but always as a result of NP degeneration. A degenerated AF shows chondroid metaplasia and ruptured and separated annular lamellae. AF degeneration has a tendency to occur at one particular site within the AF, most of the time the changes are found in the dorsal or dorsolateral AF and hardly ever in the ventral AF. Aside from these lesions, the AF may look completely healthy(Smolders et al., 2013).

In CD dogs IVD degeneration progresses quickly and the result can be a dorsal herniation of the NP as early as 2 years of age. This herniation has a sudden onset and explosive character.(Olby et al., 2004; Smolders et al., 2013) The dorsomedian or dorsolateral AF and the dorsal longitudinal ligament completely rupture. This leads to extrusion of the degenerated NP through all layers of the ruptured AF into the vertebral canal. Sometimes extruded disc material is dispersed, but most of the time the NP tissue remains located in close proximity to the affected disc space. This type of herniation is known as Hansen type I herniation and generally occurs in the cervical and thoracolumbar spine(Brisson, 2010; Smolders et al., 2013).

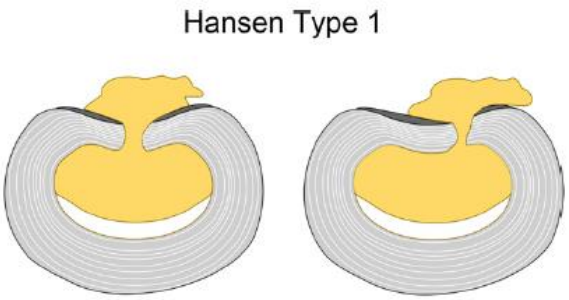

Figure 4: Schematic picture of a type I herniation of an intervertebral disc (IVD). Type I IVD herniation involves complete rupture of the dorsomedian (left) or dorsolateral (right) annulus fibrosus (AF, grey) and dorsal longitudinal ligament (DLL, dark grey) with extrusion of degenerated nucleus pulposus (NP) material (yellow). Type I IVD herniation is commonly observed in chondrodystrophic dog breeds(Smolders et al., 2013).

Non-chondrodystrophic dogs

In NCD dogs, IVD degenerative disease develops later in life, around 6–8 years of age. The macroscopic changes of the NP are comparable to those in CD dogs. The alteration from a gelatinous to a dehydrated NP usually occurs in single IVDs in the caudal cervical and lumbosacral spine, but the thoracolumbar spine can be affected as well. Some NCD breeds that are often affected by IVD degenerative disease are the German Shepherd, Dobermann, Rottweiler, Labrador Retriever, Dalmatian, as well as mixed breed dogs (Brisson, 2010; Cherrone, Dewey, Coastes, & Bergman, 2004; Smolders et al., 2013).

In NCD dogs, the notochordal cell remains the main cell type of the NP during life.(Cappello et al., 2006; Erwin et al., 2011; Johnson et al., 2010) However, age-related changes may arise, known as 'slow maturation'. In this maturation process, the NP is divided into distinct lobules of notochordal cells by collagenous strands. The notochordal cells may undergo degenerative changes and they acquire a more fibrocyte-like morphology (fibroid metamorphosis) (P. N. Bergknut, 2011).

In NCD dogs, the degenerative changes of the AF often occur simultaneously with those of the NP, but may even occur before changes in the NP are seen. Degeneration has a gradual character in NCD breeds and generally leads to partial rupture of the AF fibers. A lesion in the AF can subsequently result in partial NP herniation. The NP migrates into the AF, which is called intradiscal protrusion. The result is bulging of the IVD and dorsal longitudinal ligament. This type of herniation is referred to as Hansen type II herniation and mainly occurs in the caudal cervical and lumbosacral spine. However, NCD dogs may also suffer from Hansen type I herniation, whereas Hansen type II herniation is also reported in CD breeds (P. N. Bergknut, 2011; Brisson, 2010; Kranenburg et al., 2013; Smolders et al., 2013).

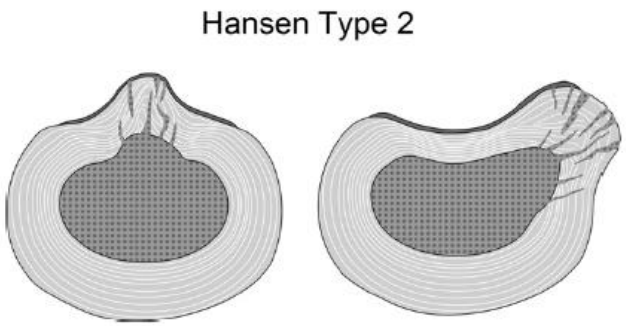

Figure 5: Schematic picture of a type II herniation of an intervertebral disc (IVD). Type II IVD herniation involves partial ruptures and disorganization of the AF (grey), and bulging of NP, AF, and DLL towards the dorsomedian (left) or dorsolateral (right) side. Type II IVD herniation is commonly observed in nonchondrodystrophic dog breeds (Smolders et al., 2013).

Clinical signs

IVD degeneration often occurs on a subclinical level, but sooner or later the degeneration may result in type I or type II herniation of the IVD. This may lead to compression of the neural structures overlying the IVD, which subsequently causes neurological deficits. Different diseases as a result of IVD degeneration are: cervical and thoracolumbar IVD herniation, cervical spondylomyelopathy, and degenerative lumbosacral stenosis.

Hansen type I IVD herniation

As discussed above, type I herniation of the IVD is characterized by local rupture of the dorsal AF and the dorsal longitudinal ligament, which leads to extruding of NP tissue into the spinal canal. IVD herniation typically occurs in the cervical and thoracolumbar area, with C2-C3 and T12-T13 or T13-L1 being the most commonly affected IVDs in CD breeds. Type I herniation generally causes acute compression of neural structures and a sudden onset of clinical signs. Clinical signs of cervical IVD herniation include acute cervical spinal pain, hyperesthesia of the neck region, muscle fasciculations or spasms, guarding of the neck, unilateral or bilateral lameness caused by lower cervical nerve root compression and sometimes ataxia with tetraparesis or tetraplegia. Dogs with thoracolumbar IVD herniation may suffer from back pain and neurological deficits, including paraparesis, paraplegia, loss of bladder function, fecal incontinence, and loss of deep pain perception. The risk of developing neurological deficits is higher for thoracolumbar IVD herniation than for cervical IVD herniation. The thoracolumbar part of the vertebral canal is more narrow than the cervical part, so neural structures get compressed more easily(Hazewinkel et al., 2013).

Hansen type II IVD herniation

As discussed above, type II herniation is caused by the simultaneous degeneration of the NP and AF, which results in bulging of the NP, AF, and dorsal longitudinal ligament. There is no extrusion of NP material into the spinal canal, but because of the bulging there may be compression of neural structures. Type II herniations can be found in the cervical and thoracolumbar spine, with C6-C7, T13-L1, L1-L2 and L2-L3 as the most commonly affected segments. Clinical signs are generally less severe than those of type I herniation and they develop more gradual. Common clinical signs of cervical type II IVD herniation include muscle fasciculations, guarding of the neck, cervical spinal pain, hyperesthesia of the neck region and unilateral or bilateral lameness caused by lower cervical nerve root compression. Thoracolumbar type II IVD herniation may cause back pain of varying severity and paraparesis. The severe signs that are seen in thoracolumbar type I herniation, such as loss of deep pain perception and paraplegia, are not seen in type II IVD herniation (Hazewinkel et al., 2013).

Cervical spondylomyelopathy (CSM)

IVD-related cervical spondylomyelopathy (CSM) involves the degeneration and type II herniation of one or more cervical IVDs, and at the same time stenosis of the cervical vertebral canal and/or hypertrophy of the interarcuate ligament. This combination of events results in compression of the cervical spinal cord. IVD-related CSM is mainly seen in large-breed dogs and the most common involved intervertebral space is C6-C7, followed by C5-C6. Clinical signs appear at an average age of 7.9 years. Doberman Pinschers are predisposed to

develop CSM. They often show a congenitally abnormal construction of the vertebral column, including vertebral canal stenosis and asymmetry of the cervical vertebral bodies. Besides, the IVDs of Doberman Pinschers are quite large, so if herniation occurs the bulging will be large as well. Sometimes degeneration occurs without resulting in clinical signs. Those asymptomatic dogs appeared to have a wider vertebral canal compared to dogs that do develop CSM. Having a small vertebral canal predisposes for developing CSM, because the risk of neural compression gets higher. Another reason why signs could remain subclinical, is that CSM may lead to either dorsiflexion or ventroflexion of the cervical spine. If dorsiflexion occurs, the compression of neural structures gets worse. Ventroflexion though, lessens the neural compression.

Dogs suffering from CSM are mostly presented with chronic and progressive clinical signs, although acute neck pain may also occur. Other clinical signs include abduction of the elbows with internal rotation of the digits, proprioceptive ataxia, spastic gait of the thoracic limbs, and extreme flexion of the elbow joints with resulting hypermetria of the thoracic limbs. Also, signs of nerve root signature affecting the thoracic limbs and uncoordinated gait with abduction of the pelvic limbs can be observed. Severely affected dogs may present with tetraparesis or tetraplegia(Hazewinkel et al., 2013).

Degenerative lumbosacral stenosis

DLSS is a multifactorial degenerative disorder of the L7-S1 spinal segment. It is seen especially in large breed dogs, with a predisposition for working dogs and German Shepherd dogs. Males are affected more often than bitches and the average age of developing DLSS is 7 years. DLSS is initiated by an abnormal motion pattern of the lumbosacral junction. This can be due to stress or to genetic or congenital abnormalities. German Shepherd dogs for example, are predisposed to have transitional vertebrae. In those dogs, L7 is fused with the sacrum either on one or on both sides, or the first two sacral vertebrae are separated. A correlation has been shown between the occurrence of transitional vertebrae and the presence of DLSS. The abnormal motion pattern may lead to IVD degeneration of the L7-S1 spinal segment. Degradation of the proteoglycans occurs which leads to dehydration and further degeneration. The spinal segment gets unstable and therefore the forces are shifted from the central axis of the IVD to the peripheral parts of the spine. This may lead to ventral subluxation of the sacrum, which subsequently affects the cauda equina. Proliferation of the surrounding soft tissue occurs, to compensate for the instability. Hypertrophy of the interarcuate ligament, epidural fibrosis and thickening of the capsules of the articular processes can be observed. Furthermore, bony proliferations arise, to compensate the forces that the IVD cannot bear anymore. The EPs thicken and osteophytes and ventral spondylosis appears. This process further impairs the nutrition of the disc. These structural failure to the disc forms a vicious cycle which eventually results in herniation, mostly type II herniation. All together this may lead to stenosis of the spinal canal and compression of the cauda equina and/or its blood supply. High pressure arises on the lateral recessus and the vertebral foramen, resulting into compression of the nerve root. Signs include difficulty standing up, sitting, or lying down, reluctance to jump or climb, dragging of toes, low carriage of the tail, posterior paresis and in extreme cases urinary and/or fecal incontinence. This causes pain, lameness and neurologic deficits. Besides, the inflammatory process may lead to ingrowth of nerves and blood vessels into the degenerated L7-S1 IVD, which contributes to the caudal lumbar pain (Meij & Bergknut, 2010).

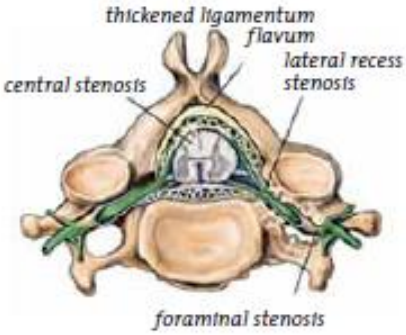

*Figure 6: Due to proliferation of soft and bony tissues, pressure arises on the vertebral canal, the foramen vertebrale and the laterale recessus.(
www.back.com/causes-mechanical-stenosis.html#).*

Inflammatory process

When cells are injured by inflammatory stimuli, their cell membrane lipids are rapidly rearranged to create a variety of biologically active lipid mediators derived from arachidonic acid. Arachidonic acid is an integral component of membrane phospholipids and serves as the major precursor for eicosanoids. Eicosanoids are synthesized by two important classes of enzymes: cyclooxygenases and lipoxygenases. Free arachidonic acid is metabolized via the COX pathway resulting in the formation of prostaglandins and thromboxanes, or via the lipoxygenase pathway resulting in the formation of leukotrienes and lipoxins. There are three COX isoenzymes (COX1, COX2 and COX3). The COX-1 isoenzyme is constitutively expressed, and is present in almost all tissues and plays an important role in maintaining hemeostasis and gastroprotection. COX-2 isoenzyme is induced under inflammatory conditions. COX-3 isoenzyme is a variant of COX-1 and is present in the cerebral cortex and heart of dogs. Arachidonic acid is metabolized by COX isoenzymes to form the prostaglandin endeperoxyde H2 (PGH2). PGH2 is subsequently metabolized by PGE synthase (PGES). Three types of PGES have been cloned. The cytosolic form (cPGES) is ubiquitous and non-inducible, whereas the microsomal PGES type 1 (mPGES-1) is involved in PGE2 synthesis during inflammation. The third form of PGES, called microsomal PGES type 2 (mPGES-2) is expressed in various cells and seems to be poorly regulated by inflammation. PGE synthases form at least 5 metabolites, and one of them is PGE2. This prostanoid is the major prostanoid produced by epithelial cells, fibroblasts and smooth muscle cells and can induce vascular permeability (McGavin, M. Donald., Zachary,James F., 2007).

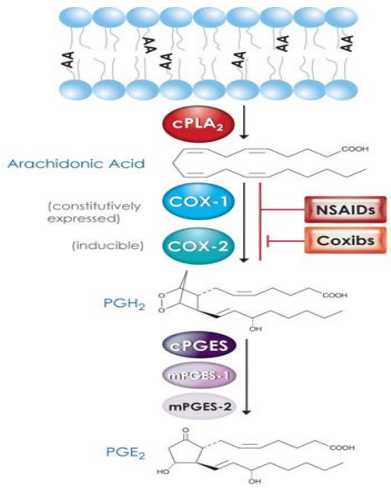

Figure 8: Schematic image of the biosynthesis of PGE2.(Tom Brock,)

Many questions still exist about the pathophysiology of IVD degeneration in dogs. However, IVD degeneration in dogs is very similar to IVD degeneration in humans(N. Bergknut et al., 2012). Studies have shown that human degenerated discs spontaneously produce increased amounts of inflammatory mediators, suggesting a pivotal role in the degenerative process of IVD diseases. A number of inflammatory mediators have been implicated in the degeneration process, including nitric oxide (NO), interleukins, matrix metalloproteinases (MMP), prostaglandin E2 (PGE2), tumor necrosis factor alpha (TNF-alpha) and a variety of cytokines. MMPs, PGE2, and a variety of cytokines have already shown to play a role in the degradation of articular cartilage. Degeneration of articular cartilage shows similarities with IVD degeneration. However, the role of inflammatory mediators in IVD degeneration has not been studied assertively(Podichetty, 2007).

Furthermore, an inflammatory reaction arises when herniation of the IVD occurs. In case of a type I IVD herniation, disc material extrudes into the spinal canal. In surgical samples of canine herniated IVDs, infiltrates revealed neutrophils and macrophages as the most common inflammatory cells(Royal, Chigerwe, Coates, Wiedmeyer, & Berent, 2009). It is supposed that an acute inflammatory reaction, which leads to swelling of the extradural tissue, could worsen the clinical signs because of compression of the dura. If the dura is damaged, inflammatory mediators may directly impair the spinal cord. In case of a type II herniation of the IVD, the integrity of the AF is decreased. Blood vessels can grow into the periphery of the intervertebral disc, leading to inflammatory changes in the AF. In some surgical samples, lymphocytes, plasma cells, macrophages and granulation tissue have been detected . This indicates a more chronic inflammatory reaction(Kranenburg et al., 2013).

Therapies for IVD degeneration

All of the current therapies to treat IVD degeneration are symptomatic and do not restore the functionality of the IVD. The most common treatments will be discussed now.

Conservative or medical treatment

Conservative treatment includes administration of analgesics. Anti-inflammatory medication is used to counter the inflammatory response and to treat the spinal pain. Corticosteroids or nonsteroidal anti-inflammatory drugs (NSAIDs) can be administered, but NSAIDs are preferred to corticosteroids(Hazewinkel et al., 2013). NSAIDs can block the activity of cyclooxygenase, which leads to a reduction in tissue prostaglandins and therefore a reduced inflammatory response and analgesia. It has also been suggested that the analgesic effect of NSAIDs may be important in recovery from a variety of orthopedic and neurologic diseases, as reduced pain may facilitate early mobilization and prevent muscle atrophy due to disuse. Side effects of NSAIDs can be gastrointestinal ulceration and perforation, coagulation disorders, and nephropathy(Levine et al., 2007b). However, NSAIDs show fewer side effects than do corticosteroids, while the analgesic and anti-inflammatory effects are the same.(Hazewinkel et al., 2013) A study performed in 2007, in which 88 dogs suffering from presumptive cervical disc herniation were assessed, showed that NSAID administration was associated with the success of medical treatment. There was no evidence in this report that glucocorticoids had a positive effect on success of medical treatment or on the QOL (quality of life) score(Levine et al., 2007a). In a similar study, in which 223 dogs suffering from presumptive thoracolumbar disc herniation were assessed, it appeared that dogs that were administered NSAIDs were more likely to have higher QOL scores when compared with those that were not administered these medications. The authors also described that

glucocorticoid administration was associated with lower QOL scores and decreased success of medical treatment(Levine et al., 2007b).

So, analgesic support is often provided by nonsteroidal anti-inflammatory drugs. However, conservative treatment includes more than the administration of analgesics alone. Exercise and physical therapy are helpful as well. Physical therapy is meant to prevent muscle atrophy due to disuse of muscles. Physical therapy leads to an improved muscle tone which subsequently promotes motion patterns. Exercise should be well controlled, because the herniating of more NP material should be prevented. Activities that could worsen the neural compression should be restricted(Brisson, 2010; Hazewinkel et al., 2013). Cage rest is often recommended to prevent continued NP extrusion through the ruptured AF, because the cage rest may allow for healing of ligamentous structures. Besides, in the rest period the extruded NP material can be resorbed which reduces the inflammation process and clinical signs. Furthermore, cage rest reduces the risk of self-trauma as a result of incoordination. However, the studies of Levine showed that cage rest duration was not significantly associated with success of the treatment or with QOL scores. Although cage rest traditionally has been considered one of most important aspects of medical treatment for disc herniation in veterinary medicine, these results indicate that long-term strict confinement is not helpful. Levine supposes that an initial period of strict cage confinement may be beneficial if it is followed by physical rehabilitation(Levine et al., 2007b). Additional treatments, such as the application of nutraceuticals and/or losing weight, are often used in conservative treatment as well. Conservative treatment is supposed to be best suited for mild cases of IVD disease(Brisson, 2010; Hazewinkel et al., 2013).

Surgical Treatment

In general, surgical therapy is recommended when clinical signs do not respond to conservative treatment, or when neurological deficits are present. The severity of neurological signs, compressive lesion(s) and pain, plays an important role in the decision making of proceeding to surgical treatment as well. The overall purpose of surgery is to lessen neural compression by removing the compressive tissues, such as the herniated parts of the IVD and hypertrophic ligaments. A variety of surgical techniques are available to decompress neural structures. Direct decompressive procedures include ventral slot/inverted cone slot, dorsal laminectomy and hemilaminectomy. Those techniques are performed for respectively the treatment of cervical disc disease (including CSM), DLSS and thoracolumbar disc disease. Another commonly performed technique is fenestration of the aberrant disc or adjacent discs which may cause problems in the future. Indirect decompressive techniques, such as distraction-stabilization/fusion, are also used as treatment for CSM and DLSS. Because with decompression some critical stabilizing structures are removed, the decompressed segments can also be re-stabilized. Multiple techniques have been developed for this purpose, including the use of bone grafts, pins, screws, and cages(Hazewinkel et al., 2013).

Ventral slot/inverted cone slot

In the case of ventral compression of the cervical spinal cord due to IVD herniation and CSM, a ventral approach is generally used. The degenerated IVD and parts of the adjacent vertebrae, are removed by making a rectangular shaped window/slot in the vertebrae and IVD (Figure 9). If IVD material is extruded into the vertebral canal, the dorsal longitudinal ligament can be removed to obtain access to the vertebral canal to remove the material. A ventral approach however makes it hard to remove lateralized and dorsally located IVD material(Hazewinkel et al., 2013).

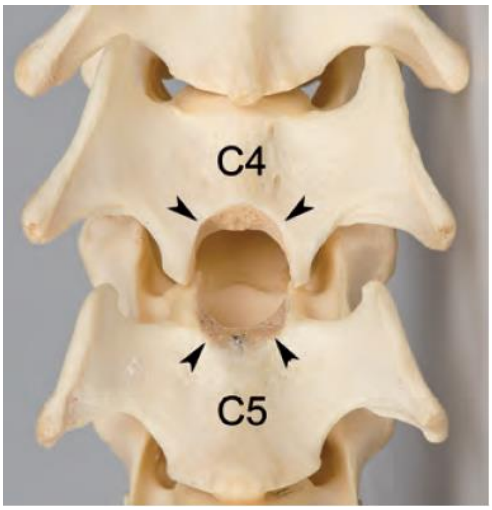

Figure 9: Ventral slot (arrowheads) of C4-C5, providing access to the cervical vertebral canal(Hazewinkel et al., 2013).

Dorsal laminectomy

Dorsal laminectomy is the primary surgical procedure for DLSS. The aim of this surgery is to decompress the cauda equine nerve roots at the lumbosacral junction. In case of nerve root compression, foraminotomy (widening of the intervertebral foramen) is applied to relieve spinal nerve compression. In patients with nerve root compression but without spinal canal stenosis, sometimes foraminotomy without simultaneous dorsal laminectomy is performed. In some cases the facet joints are removed, but this should only be done when absolutely necessary, because removal of the facet joints increases lumbosacral instability. Improvement of clinical signs after DLSS surgery has been reported in 69-93% of the surgically treated cases. However, in the long run clinical signs may reoccur in 3-37% of the patients that underwent surgery. This can be explained by the fact that lumbosacral instability can arise after surgery, which in turn contributes to degenerative changes in the lumbosacral spinal segments(Hazewinkel et al., 2013).

Figure 10: Dorsal laminectomy of L7-S1, providing access to the vertebral canal and the L7-S1 intervertebral disc(*)(Hazewinkel et al., 2013).

Hemilaminectomy

Hemilaminectomy is performed to decompress the thoracolumbar spine. Hemilaminectomy is a technique similar to dorsal laminectomy; however, it involves a lateral approach and only the removal of the lamina on one side. Hemilaminectomy is preferred to dorsal laminectomy for treating thoracolumbar IVD patients, because the dorsal vertebral lamina does not have to be removed (Figure 10). This results in less instability of the thoracolumbar spine. Furthermore, it results in a significantly higher rate of postoperative neurologic improvement. Positive clinical outcome has been associated with complete removal of the compressive disc material rather than simple vertebral canal decompression. Additional fenestration of the diseased IVD is commonly performed to prevent further extrusion of IVD material through the ruptured AF(Hazewinkel et al., 2013).

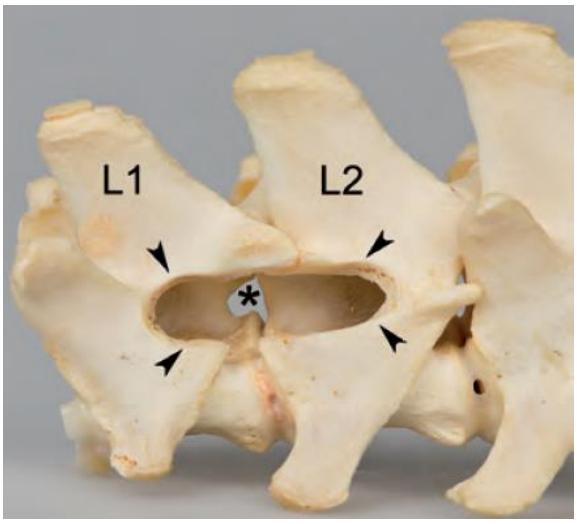

Figure 11: Left hemilaminectomy of L1-L2. After burring through the left lateral pedicle wall (arrowheads), disc material located in the vertebral canal can be removed(Hazewinkel et al., 2013).

IVD fenestration
Fenestration involves removal of degenerated NP material through a small incision in the AF. In CD patients, which usually show degeneration of multiple spinal segments, fenestration of thoracolumbar IVDs adjacent to the surgical lesion can be performed to prevent future IVD herniation. It appears that herniation reoccurs less often after surgery with simultaneously performed prophylactic fenestration than after surgeries without prophylactic fenestration. A disadvantage of prophylactic fenestration is that it may induce spinal instability and postoperative morbidity. Nevertheless, although an IVD is degenerated, it still has a biomechanical function. Therefore the use of prophylactic fenestration is still discussed(Hazewinkel et al., 2013).

Vertebral stabilization techniques
Diverse distraction/fusion techniques are developed, mainly for the treatment of CSM, but also for the treatment of DLSS. Spinal or cervical segments can be stabilized by insertion of pins or screws into the vertebrae and the vertebrae can be fixated with for example a polymethyl metacrylate (PMMA) bridge. Stabilization prevents degeneration of the decompressed spinal segment, but an important disadvantage of stabilization is that it may lead to degeneration of the nearby spinal segments. This phenomenon is called adjacent segment disease.

All the above described treatments are symptomatic and do not restore the functionality of the IVD. Nowadays new technologies are discussed to restore the functionality of the IVD following decompression. Recently, a new, biocompatible hydrogel NP prosthesis (NPP) has been developed which can be inserted in the IVD through a small opening in the AF. In situ the prosthesis expands and fills up the entire NP cavity which is created after nuclectomy. The NPP is developed to mimic the dimensions and shape of the natural NP. More research is needed to investigate whether this technique can be used in the future for dogs suffering from IVD disease(Hazewinkel et al., 2013).

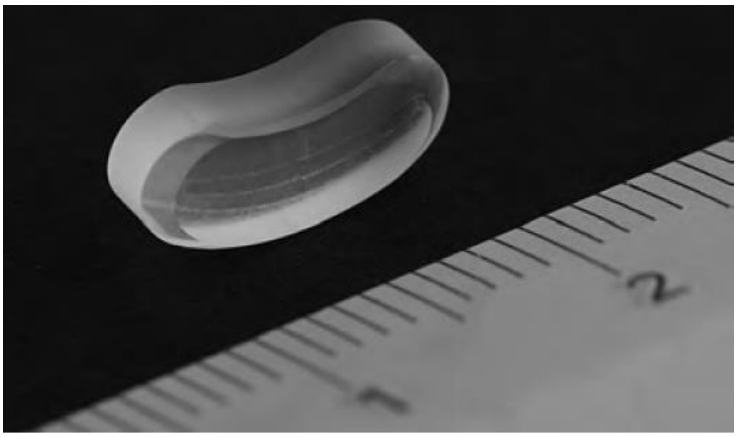

Figure 12: A hydrogel nucleus pulposus prosthesis (scale is in cm)(Hazewinkel et al., 2013).

Regenerative strategies
More ideally than restoring the functionality of the intervertebral disc with an NP prosthesis, would be to achieve regeneration of the degenerated IVD tissue and returning the IVD to its healthy state. To achieve this, degenerative processes should be prevented, inhibited or reversed. At the same time, synthesis of the extracellular matrix (ECM) should be stimulated while degradation of the ECM should be decreased or, even better, reversed. Multiple strategies for biological repair of the degenerated IVD are discussed, including the use of growth factors and anti-catabolic/anabolic agents, gene therapy, and cell-based strategies.

Examples of such strategies include the application of tissue inhibitor of metalloproteinase (TIMP)-1, and bone morphogenetic protein (BMP), which are respectively anti-catabolic and anabolic agents. As discussed earlier in this introduction, the disappearance of notochordal cells from the NP is involved in initiating degeneration. Notochordal cells have a positive effect on the activity and homeostasis of surrounding chondrocyte-like cells. Notochordal cells have gained increased attention in the development of regenerative strategies, because they may act as a potential NP progenitor cell. Regenerative strategies may become suitable treatment strategies, specifically in patients with early IVD degeneration(Hazewinkel et al., 2013).

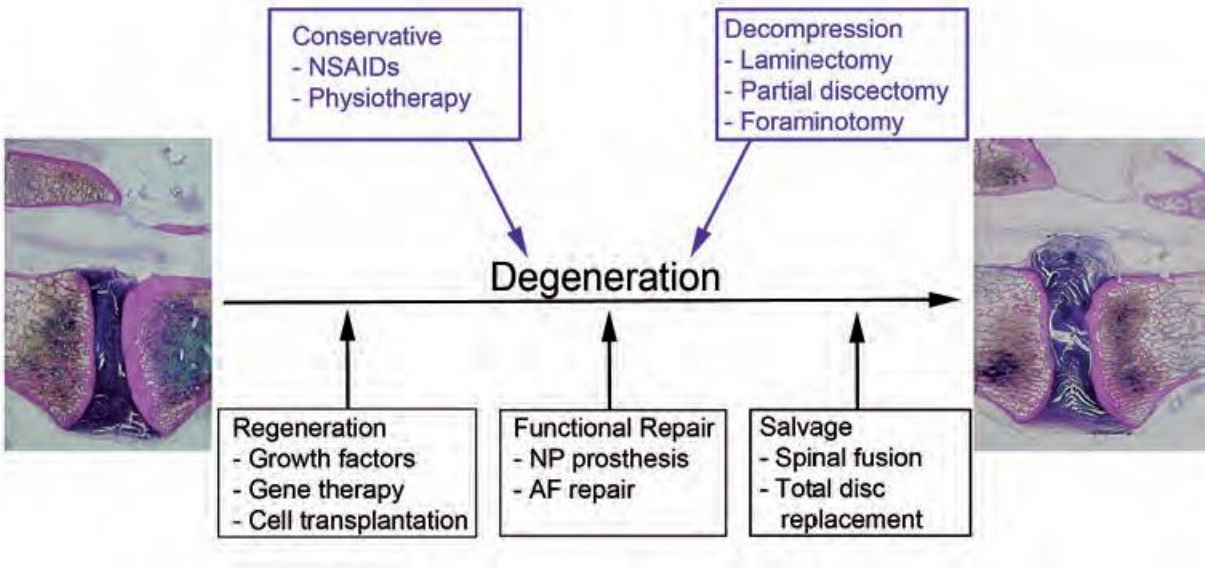

Figure 13: Current and new treatment strategies for intervertebral disc degeneration. Current treatment strategies (purple boxes and letters) include conservative therapy and surgical therapy. The new treatment strategies (black boxes and letters) can be applied at different stages of intervertebral disc degeneration, with intervertebral disc regeneration being applied in early-stage degeneration, functional repair being applied in intermediate-stage degeneration, and salvage procedures being applied in late-stage degeneration/disease(Hazewinkel et al., 2013).

Immunohistochemical staining

In most cases routine histological staining (e.g. hematoxylin and eosin (H&E)) provides adequate information about the structural details of cartilage samples. However, sometimes additional information on physiological and pathological processes in the tissue is desirable and immunohistochemical staining may be required(An, Yuehuei H., Martin,Kylie L., 2003).

How does immunohistochemical staining work?

In general, all immunostaining techniques are based on the binding of a specific antibody to a target antigen. The variable site of the antibody binds to the target antigen, while the invariable end of the antibody remains unbound. The antigen-antibody complex can then be visualized by binding the unbound invariable end of the antibody to a secondary antibody system. The invariable end of the antibody contains species-specific protein structures, that serve as targets for the secondary system. Primary antibodies that are generated in rabbits, form a complex with an anti-rabbit secondary system. The complex of the primary and secondary antibody can be visualized by the reaction of an enzyme coupled to the secondary antibody. Those enzymes (for example peroxidase or alkaline phosphatase) will give a color

reaction if the right substrates are added. Recent developments made it possible to strengthen the resulting signals, by forming complexes of the antibody systems with large signals. This results in a higher test sensitivity(An, Yuehuei H., Martin,Kylie L., 2003).

Avidin-biotin immunohistochemistry

The peroxidase techniques are commonly used techniques for the localization of a broad range of antigens. Several peroxidase techniques exist and they differ in type and size of the resulting signal, and therefore they vary in sensitivity. Recent developments such as reinforcement of the signal have reduced the concentration of antibodies needed for the staining. For example, the avidin-biotin-complex method (ABC method) makes use of the high affinity of avidin (from chicken egg) or streptavidin (from Streptomyces avidinii) to biotin. The biotin molecule can be easily conjugated to antibodies and enzymes. Biotin can be coupled to the secondary antibody without changing the structure of the secondary antibody. This antibody-biotin complex is then coupled to avidin molecules that are already linked to peroxidase. So, the secondary antibody coupled to biotin forms a link between the primary antibody and an avidin-biotin-peroxidase complex. This method is also referred to as the LAB (labelled avidin-biotin technique)(An, Yuehuei H., Martin,Kylie L., 2003; Kumar, 2009).

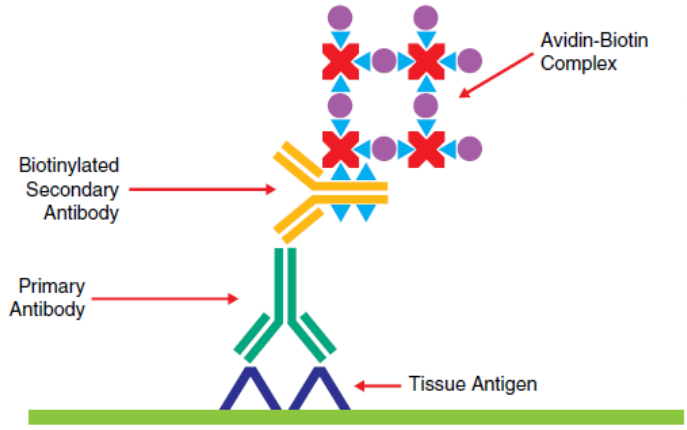

Figure 14: Avidin-biotin complex (ABC) method (indirect method)(Kumar, 2009).

The LSAB technique is a technique similar to the LAB, but it makes use of streptavidin instead of avidin. A biotinylated secondary antibody forms a complex with streptavidin molecules that are already linked to peroxidase.

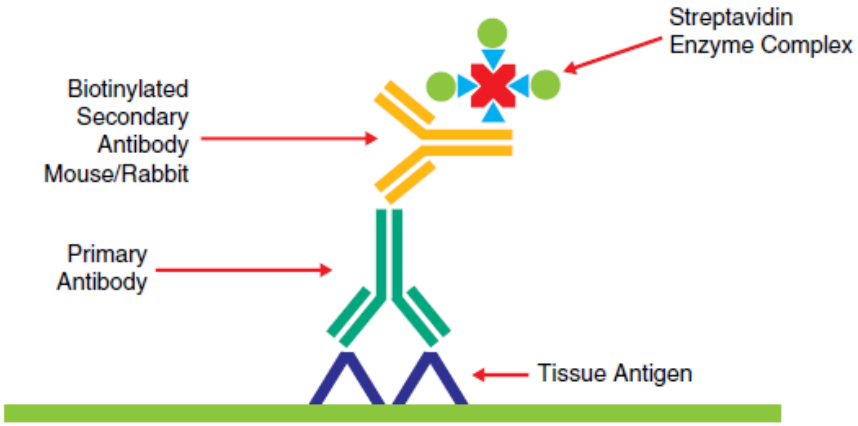

Figure 15: Labeled Streptavidin-Biotin (LSAB) method(Kumar, 2009).

In both methods, a single primary antibody is associated with multiple peroxidase molecules, and because the large enzyme-to-antibody ratio, a considerable increase in sensitivity is achieved(An, Yuehuei H., Martin,Kylie L., 2003; Kumar, 2009).

Polymer-Based immunohistochemistry

Many of these streptavidin-biotin methods are still in use, but those methods have some limitations. The presence of endogenous biotin in tissues can lead to significant background staining. Formalin fixation and paraffin embedding reduces the expression of endogenous biotin, but residual activity may still be observed. The levels of endogenous biotin in frozen tissue sections are even higher than those encountered in paraffin-embedded specimens. Methods to block endogenous biotin exist, but they make the method more complex. Because of these limitations, polymer-based immmunohistochemical methods that are independent of biotin have been introduced. These methods make use of a polymer backbone to which multiple antibodies and enzyme molecules are conjugated. In the Enhanced Polymer One Step system (EPOS), as many as 70 enzyme molecules and about 10 primary antibodies can be conjugated to a dextran backbone. In this way, the whole immunohistochemical staining procedure can be accomplished in a single step. However, a disadvantage of this method is its limitation to a select group of primary antibodies provided by the manufracturer(Kumar, 2009).

To overcome this limitation, a new type of dextran polymer (EnVision) was introduced. This polymer system contains a dextran backbone to which multiple enzyme molecules are attached. In contrast to EPOS, which contained primary antibodies, the EnVision system contained secondary antibodies with anti-mouse Ig and anti-rabbit Ig specificity. So, this reagent can be used to detect an tissue-bound primary antibody of mouse or rabbit origin. The sensitivity of this method compared to LSAB and ABC methods is comparable or even higher in most cases(Kumar, 2009).

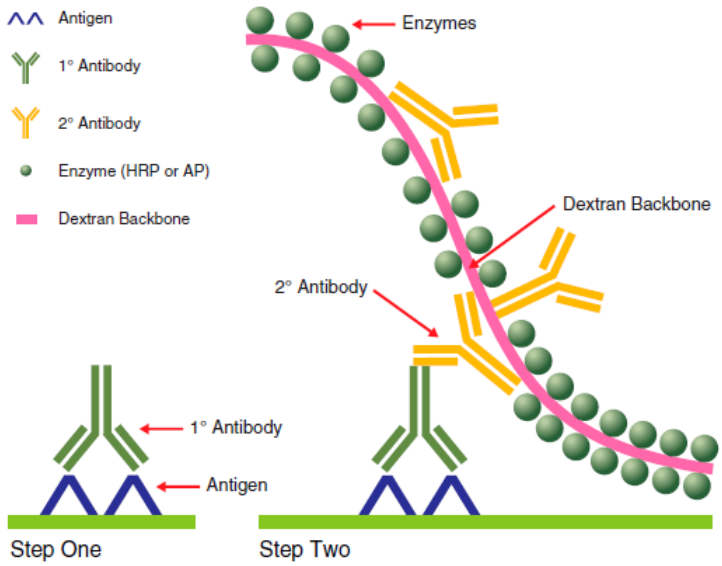

Figure 16: Two-Step Polymer Method (EnVision)(Kumar, 2009).

Section Preparation

Paraffin Embedding

To be able to perform an immunostaining, tissue needs to be fixated on a slide. Different embedding procedures exist, but the most common procedure used for long-term maintenance of tissue, is fixation in formaldehyde followed by embedding in paraffin wax. Embedding in wax has several advantages over using the frozen section technique. First, tissues can be stored for a longer period of time. Furthermore, wax-embedded tissue can be sectioned much easier than frozen tissue. In tissues that contain calcifications or bone, which are difficult to cut, the wax-embedding technique is recommended. Wax-embedding allows to cut thin sections and tissue structures and morphological details are well maintained. A disadvantage of the wax-embedding technique are the chemical changes that may influence antigen preservation, which can cause problems in performing immunochemical stainings. Therefore, new antibodies need to be pretested extensively(An, Yuehuei H., Martin,Kylie L., 2003).

Decalcification

When cartilage tissue samples contain calcifications or bone material, a decalcification step is preferable to obtain sections of 4 – 6 µm. This decalcification can be performed after fixation of the tissue by the use of chelating agents, most often by use of 0,1M ethylenediaminetetraacetic acid (EDTA). Those agents have no influence on the structure of antigens, and thus do not alter methods for antigen retrieval. Such a mild decalcification step may give specific information about for instance the end plates of the intervertebral discs. However, when people are interested in information about pathological calcifying processes in cartilage tissue, decalcification is not a good option because it may suppress these information(An, Yuehuei H., Martin,Kylie L., 2003).

Monoclonal antibodies

Monoclonal antibodies are a homogeneous population of immunoglobulin directed against a single epitope. The antibodies are generated by a single B-cell clone from one animal and are therefore immunochemically similar.

Figure 17: A given clone of monoclonal antibodies reacts with a specific epitope of an antigen(Kumar, 2009).

Monoclonal antibodies are most commonly produced in mice and rabbits. The animals are immunized using intraperitoneal injections of an immunogen. Mice are boosted every two weeks over a period of two months and rabbits for over a period of two to four months. The animals immune response is monitored through repeated testing of the serum. By the time an acceptable immune response is achieved, the animal is euthanized. The B-lymphocytes are

isolated from the spleen and fused with an immortal cell line (myeloma cells). In this way the capacity of the B-lymphocytes to produce specific immunoglobulin is combined with the immortality and indefinite growth in culture of the myeloma cells. This obtained fused cell line is called a hybridoma. A stable clone is isolated from the hybridoma cell line, with a high antibody production capacity. For production of tissue culture supernatant, the hybridoma cell line is cultured in multiple tissue culture flasks. Large scale hybridoma growth and antibody generation can be achieved by adding a bioreactor. A bioreactor frequently replenishes the cells with fresh media, which promotes growth for the development of concentrated amounts of antibody. Another possibility is to use ascites fluid, because ascites fluid has a very high concentration of antibody compared to tissue culture supernatant. Ascites fluid is produced by injecting the hybridoma into the peritoneal cavity of an animal (usually a mouse). The mouse forms a tumor and secretes immunoglobulins into the peritoneal cavity. Ascited fluid is then extracted. Next to the ethical considerations, an disadvantage of this method is that the fluid will contain contaminating antibodies. While the majority of monoclonal antibodies are produced in mice, a growing number of rabbit monoclonal antibodies are being manufactured. The use of rabbits for monoclonal antibody production confers some advantages over mouse monoclonals. Rabbits are reported to have more diverse epitope recognition than mice and they have an improved immune response to small-sized eptitopes. Furthermore, rabbits may generate antibodies with higher affinity and enhanced binding properties. Mouse hybridomas however tend to generate a higher yield of immunoglobulin than rabbit hybridomas and the mouse hybridoma cell lines are typically more stable in culture.

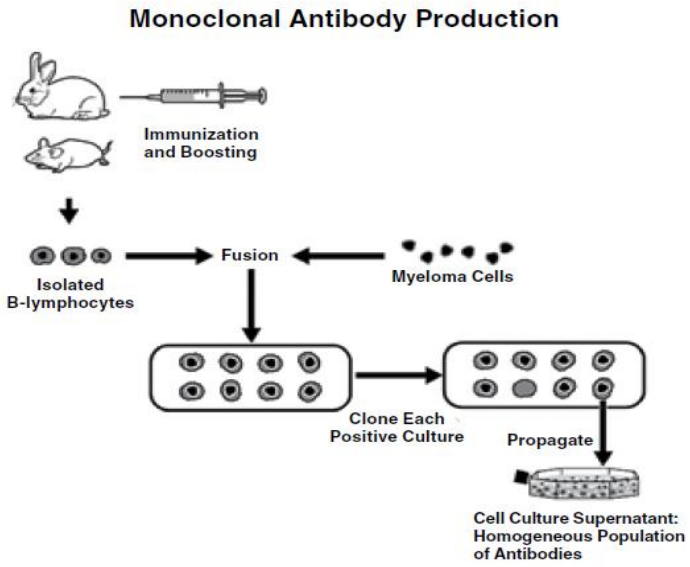

Figure 18: Image: The process of monoclonal antibody production(Kumar, 2009).

Optimizing the staining protocol

In immunohistochemistry, staining quality is influenced by many factors, including antibody titer and antibody dilution, incubation time and incubation temperature. In each specific staining, these factors might have to be changed, to achieve optimal staining. The aim of optimization is to improve the strength and specificity of the signal, but in the meantime as less as possible background staining is wanted. Some factors that influence staining quality will be discussed below.

- Antibody titer and antibody dilution

Optimum antibody titer is achieved with the highest dilution of an antiserum or a monoclonal antibody, providing the most specific staining with minimum background staining. This highest dilution is determined primarily by the absolute amount of specific antibodies present. This absolute concentration frequently forms the basis for making required antibody dilutions, because antibody titer and antibody dilution are related factors. An optimal antibody dilution is also governed by the intrinsic affinity of an antibody. If the antibody titer is held constant, a high-affinity antibody will react faster with the tissue antigen and give more intense staining within the same incubation period than an antibody of low affinity and so antibody dilution can be changed. For monoclonal antibodies, antibody titers may vary from 1:10 to 1:1000 for monoclonal antibodies in cell culture supernatants, and up to 1:1000.000 for monoclonal antibodies in ascites fluid. Correct antibody dilutions will contribute to the quality of staining. Often a manufacturer offers ready-to-use reagents, or recommends dilution ranges compatible with other variables such as method, incubation time and temperature. If this information is not provided, optimal working dilutions must be pretested. Correct dilutions are best determined by first selecting a fixed incubation time and then by performing a staining to test series of experimental dilutions. The staining that shows the most specific and intense signal in the presence of minimal background staining, turns out to the best working antibody dilution(Kumar, 2009).

- Antibody incubation

- Incubation time

Incubation time, incubation temperature and antibody titer/dilution are interdependent factors. There is an inverse relationship between incubation time and antibody titer: the higher the antibody titer, the shorter the incubation time required for optimal results. However, as discussed above, in most cases a incubation time is selected first and then the optimal antibody dilution is determined. Incubation times for the primary antibody may vary within up to 24 hours. For an antibody to react strong enough with the tissue antigen in a short period of time, the antibody must have a strong affinity. Besides, the concentration of the antibody and the reaction milieu need to be optimal. Primary antibody incubations with a 24 hour duration would be cheaper in use, because then higher dilutions of the antibody can be used. Low concentrations of antibodies, or antibodies with low affinity must be incubated for long periods to reach saturation of an antigen with antibody. Incubation times incoherent to the other influencing factors, may lead to variations in staining quality and misinterpretation of results.

- Incubation temperature

Because antigen antibody reactions take place more quickly at 37ºC compared with room temperature, some researchers prefer incubation at these higher temperatures. Higher incubation temperatures allow for higher dilution of the antibody and a shortened incubation time. However, it is not known whether an increase in temperature promotes only the antigen antibody reactions, or also affects background staining. A temperature of 4ºC is frequently used in combination with overnight or longer incubations. Slides incubated for longer period, or at 37ºC should be kept in a humidity chamber or wetted with moist paper to preventdehydration(Kumar, 2009).

- Antigen Retrieval

As discussed above, most of the tissue samples are fixed in formalin and then embedded in paraffin. Fixation in formalin preserves tissue morphology, but alters the three-dimensional structure of tissue proteins. This change may modificate the antigen’s epitopes. When an epitope is lost, the antigen is no longer able to react with the antibody. Therefore, the epitope first has to be repaired prior to performing an immunohistological staining. Antigen retrieval

influences antigen-antibody binding and helps in optimizing the signal and minimizing the background. Different retrieval protocols exist as well as different retrieval buffers. The composition and the pH of retrieval buffers are essential for optimal retrieval. Antigen-antibody binding can also be influenced by retrieval time, so for new antibodies it is recommended to examine which antigen retrieval solution and time are best to optimize signal and minimize background(Kumar, 2009).

The staining procedure

The enzymology of the staining procedure

Immunoenzymatic staining methods use enzyme substrate reactions to convert colorless chromogens into colored end products. Horseradish Peroxidase (HRP) is an enzym which is isolated from the root of the horseradish plant. The active site of HRP is an iron containing heme group (hematin). HRP activity in the presence of an electron donor first results in the formation of an enzyme substrate complex, and then in the oxidation of the electron donor. The hematin of HRP forms a complex with hydrogen peroxide (H2O2) and decomposes to water and oxygen. The electron donor is the driving force in the ongoing catalysis of H2O2 Various electron donors exist, and they have in common that they become colored products when they are oxidized. For that reason, they are called chromogens. Besides, chromogens become onsoluble when they get oxidized. Those characteristics make electron donors useful in immunohistochemistry. The DAB chromogen (3,3'diaminobenzidinetrahydrochloride) is a popular choice for signal generation with peroxidase-based immunohistochemical detection systems. DAB is an electron donor which produces a brown, highly insoluble end product. DAB has been classified as a potential carcinogen and therefore should be handled with care(Kumar, 2009).

Endogenous enzyme blockers

As discussed above, horseradish peroxidase is one of the most common used enzyme activitity used to generate chromogenic signals in immunohistochemistry. However, horseradish peroxidase is also encountered as endogenous activity in a variety of cellular and tissue specimens. Endogenous enzymes are found for example in red blood cells, granulocytes, monocytes, eosinophils, hepatocytes, muscles and kidneys. If the endogenous enzymes are similar in specificity to the enzymes used in the immunohistochemical detection system, the endogenous activity can be produce false-positive signals that interfere with, and even overwhelm, the signals from the immunohistochemical reactions. Enzyme blockers are used to inhibit the activity of such endogenous enzymes within cells and tissue specimens. Simple reagents may be used to completely block these endogenous enzymes by either competitive inhibition or acid inactivation. In general, enzyme blockers are applied prior to the addition of antibody reagents in the staining protocol(Kumar, 2009).

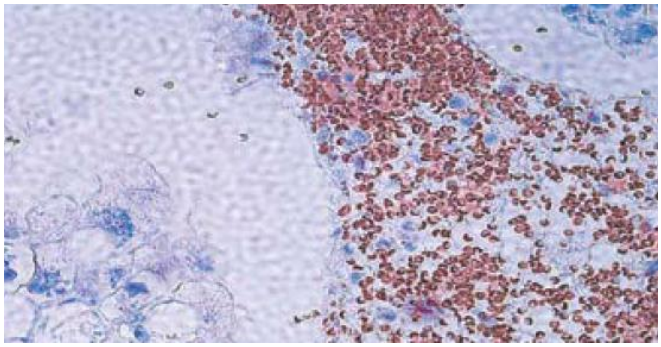

Figure 19: Example of endogenous peroxidase in red blood cells of kidney stained with DAB(Kumar, 2009).

TBS-BSA block

In aqueous media, hydrophobic interactions between macromolecules occur when surface tensions are lower than that of water (Van der Waals forces). These interactions arise through the fluctuating dipolar structure within these macromolecules. Most of the proteins show hydrophobicity, but the degree in which they do can differ. Hydrophobicity is caused primarily by the side chains of the amino acids phenylanine, tyrosine and tryptophan. These amino acids tend to link to one another, because of their lower attraction for water molecules. As a result, water is eliminated from the molecule. Hydrophobicity gives stability on the tertiary structure of peptides and can also exist between different protein molecules. Besides, it also confers stability to formed immune complexes in immunohistological staining, which may cause background. The most widely used manner to reduce background due to hydrophobic interaction is to use a protein blocking solution. This can be done either in a separate step, or by adding the protein blocking solution to the antibody diluents. A protein blocking solution only works if the locking protein is a type that can compete effectively with IgG for hydrophobic binding sites. The solution should contain proteins identical to those present in the secondary antibody, but not to those in the primary antibody, in order to prevent nonspecific binding of the secondary antibody. When the blocking is done in a separate step, this should be done prior to application of the primary antibody. The most common way to reduce non-specific binding due to hydrophobic interaction, is adding one percent bovine serum albumin (BSA) to the primary antibody diluents(Kumar, 2009).

Wash Buffers

Wash buffers are used to remove excess reagents from the specimen after each incubation step in the assay protocol, to prevent non-specific reagent binding. Commonly used wash buffers are Tris-buffered saline (TBS) and phosphate-buffered saline (PBS). When conditions require very high specificity reactions, an increase in the saline and detergent content of the wash buffer can be used to minimize non-specific binding. The addition of high concentrations of salts and detergents (for example Tween 20) to wash buffers will significantly reduce the non-specific binding of many immunohistochemical reagents. Tris(hydroxymethyl)aminomethane-based wash buffers are often utilized in combination with the non-ionic determent Tween 20. Tris-buffered solutions are pH-sensitive. PBS is relatively inexpensive compared to Tris-based buffers. However, in some cases PBS can cause more nonspecific staining, and PBS might reduce the specific binding abilities of certain monoclonal antibodies(Kumar, 2009).

Tissue Controls

Many factors may influence an immunohistochemical staining, including day-to-day variations in temperature and variations due to the conditions of reagents applied on a particular day. It is important to include tissue controls for verification of immunohistochemical staining results.

- Positive tissue controls

Positive tissue controls are needed to prove that proper staining techniques have been used and that antigen retrieval has been carried out correctly. Positive tissue controls verify that all reagents were applied and were working well, and they indicate whether the proper incubation time and temperature were used. These controls are also indicative of properly prepared tissue. Positive tissue controls should be prepared in the same manner as patient samples. Each set of test should contain one positive tissue control. Preferably, the positive control should contain a range of weak to strongly positive reactivity. Another possibility is to use a weakly positive sample as positive tissue control. In this way the positive control gives the

best information to assess whether the staining reaction is too weak or too strong. The results from the samples should be considered invalid if reaction fail to occur in the positive tissue.

- Negative tissue controls

Just as in positive controls, tissue used for negative controls should be prepared in the same manner as the patient samples, except for the fact that the negative tissue controls should not contain the specific antigen which is tested. If the negative controls show positive staining, this could indicate a lack of specificity of the antibody or it indicates nonspecific background staining. This means that the procedure needs to be further optimized(Kumar, 2009).

Pfirmann score

Many similarities between canine and human IVD degeneration exist(HANSEN, 1951). In both species, the diagnosis of IVD degeneration related diseases can be difficult and requires diagnostic imaging. The only diagnostic modality currently available to evaluate the status of an IVD itself in vivo is magnetic resonance imaging (MRI). Sagittal T2-weighted MR images are most appropriate for evaluation of IVD degeneration, because those scans show the glycosaminoglycan and water content of the disc(P. N. Bergknut, 2011). In literature a correlation is described between decrease in GAG and water content and higher Pfirrmann scores(N. Bergknut et al., 2012)/ These days, research is focusing more and more on regenerative treatment strategies to attain functional repair or even regeneration of the degenerated intervertebral disc. Therefore, early identification of the degenerative process is required and reliable and accurate diagnostic methods and grading systems are needed(P. N. Bergknut, 2011).

The Pfirrmann system is the most common used system to grade human IVD degeneration on the basis of magnetic resonance imaging (MRI) findings(Kettler & Wilke, 2006; Pfirrmann, Metzdorf, Zanetti, Hodler, & Boos, 2001). It is based on the system proposed by Thompson et al. for grading gross pathological changes in intervertebral discs(Pfirrmann et al., 2001; Thompson et al., 1990). Pfirrmann described this grading system in form of a simple algorithm using contemporary MRI technique. This grading system and algorithm are based on MRI signal intensity, disc structure, distinction between nucleus and annulus, and disc height. The system has a high intra- and interobserver reliability and provides a standardized and reliable assessment of MRI disc morphology for clinical and for research purposes. A standardized nomenclature in the assessment of disc alterations is required for comparing data from different investigations(Pfirrmann et al., 2001). Bergknut et al. validated the Pfirrmann grading system in dogs. Their study results showed that the Pfirrmann system was highly reproducible for grading IVD degeneration at all spine locations in dogs of various breeds and ages. Moreover, higher Pfirrmann scores were associated with chondrodystrophic breeds and also with increasing age. A disadvantage of this scoring system is, that it uses a categorical scale and the cut-off point between two categories is not always clear(N. Bergknut et al., 2011).

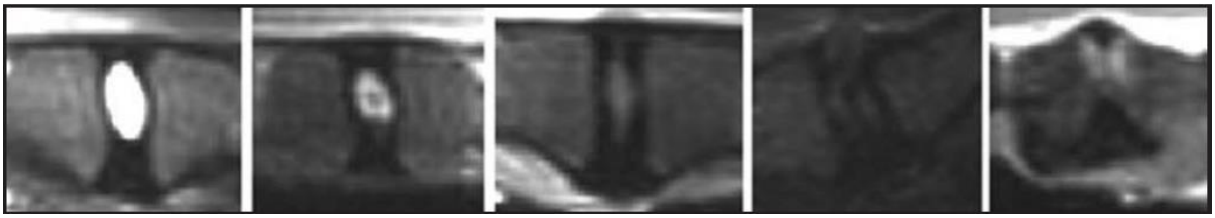

Figure 20: Midsagittal T2-weighted MRI images of IVDs obtained from representative dogs. The images show Pfirrmann grades from 1 (left) to 5 (right)(N. Bergknut, Grinwis et al., 2011).

Grade	Structure	Distinction between NP and AF	Signal intensity	Height of intervertebral disc
I	Homogenous, bright white	Clear	Hyperintense, isointense to CSF	Normal
II	Inhomogeneous with or without horizontal bands	Clear	Hyperintense, isointense to CSF	Normal
III	Inhomogeneous, gray	Unclear	Intermediate	Normal to slightly decreased
IV	Inhomogeneous, gray to black	Lost	Intermediate to hypointense	Normal to moderately decreased
V	Inhomogeneous, black	Lost	Hypointense	Collapsed disc space

NP= nucleus pulposus; AF = annulus fibrosus; CSF=cerebrospinal fluid

Table 1: Description of the MRI-based grading system used to classify IVDs in dogs ((N. Bergknut et al., 2011).

As depicted in table 2, the Pfirrmann grading system focuses only on changes in the structure of the disc itself (signal intensity, disc structure, NP and AF distinction, and disc height). Changes associated with IVD herniation, such as the occurrence of bulging, protrusion or extrusion, are not included in the scoring system(P. N. Bergknut, 2011).

Aim of the Study

The goal of this research is to investigate whether the PGE2 levels in IVDs of dogs suffering from chronic low back pain, are correlated with higher grades of disc degeneration.
The readouts of this study will be:

1) Primary readout: PGE2 in the NP and the AF of the IVDs.
2) Secondary readout: COX-2 protein expression on histological samples

Why would we investigate this?
Elevated levels of PGE2 are associated with IVD degeneration. Thus far it is not known if higher PGE2 levels are correlated with higher grades of disc degeneration. Even more, we do not know what levels in degenerating/aging IVDs are considered physiological and which levels should be considered as pathological. Perhaps, the level PGE2 we measure is absolutely normal and needed for the physiological function of the aging IVD. In that case, COX-1 is responsible for this PGE2 level(van Dijk, Potier, Licht, Creemers, & Ito, 2014).

Other secondary readout parameters:
Glycosaminoglycans (GAGs), DNA and protein content in the NP and AF tissue

Why would we investigate this?
It is interesting to know exactly what happens to the matrix composition of the IVD. By measuring the GAG content, we get to know more about the different stages of degeneration. By measuring DNA levels, we are able to have an idea on the amount of cells in the sample. PGE2 levels, GAG and DNA content will be corrected for wet weight of the sample, to be able to compare samples that have different sizes.

Hypothesis
H0 = There is no significant evidence for a correlation between higher grades of disc degeneration and increased PGE2 levels in the NP and the AF of dogs suffering from chronic low back pain.

H1 = There is significant evidence for a correlation between higher grades of disc degeneration and increased PGE2 levels in the NP and the AF of dogs suffering from chronic low back pain.

- I expect the PGE2 levels in the NP and the AF of dogs suffering from chronic low back pain will be increased.
- In the case of elevated PGE2 levels in discs with a higher grade of degeneration, I also expect to find an increased COX-2 level in discs with a higher grade of degeneration. I expect the concentration of glycosaminoglycans (GAGs) to be decreased in the NP and increased in the AF in discs with a higher grade of degeneration.
- I expect to find higher DNA levels in herniated NPs and AFs, as these will contain relatively more cells and less matrix due to the inflammation process.

Material and Methods

Experimental design

In vitro study, prospective study.

Study population and collection of materials

Most of the IVD tissue used in this study was collected from canine patients that underwent surgery (ventral slot, inverted cone slot, dorsal laminectomy or hemilaminectomy) at the University Clinic for Companion Animals in Utrecht. 41 AFs and 46 NPs were collected, coming from different locations within the vertebral column, from a total of 65 client-owned dogs.(HANSEN, 1952) The dogs were of various breeds, ages, and gender. Clinical data were retrieved from the hospital database. On the basis of earlier publications the dogs were grouped as CD or NCD. Our samples included 31 NCD dogs and 34 CD dogs. All disc samples were instantly placed in liquid nitrogen and stored in the Veterinary Biobank at -80ºC until they were further processed. During specimen processing, the investigators were unaware of associated clinical and anatomic data. After tissue processing, samples were divided in herniated or non-herniated groups.

Pfirmann scoring

In all dogs MRI was performed prior to surgery. Sagittal MR images were reviewed by 2 persons independently of one another and without prior knowledge of surgical findings. All the sample IVDs were graded by using the Pfirmann grading system. The samples were classified in groups on the basis of their Pfirrmann score in combination with NCD/CD classification. The samples in the 1NCD group originate from 4 laboratory dogs, from which 10 AF samples and 9 NP samples were collected coming from different locations within the vertebral column. Table 2a and 2b represent the number of AF and NP samples in every group. After tissue processing, the hospital database was consulted if herniation occurred. Only type I herniated samples were included into the herniation group. Table 3a and 3b represent the number of samples in every group divided in herniated samples and non-herniated samples.

Group	Number of AF samples
1NCD	10
2NCD	7
2CD	7
3NCD	6
3CD	6
4NCD	10
4CD	5

Table 2a: Number of AF samples in every group

Group	Number of NP samples
1NCD	9
2NCD	7
2CD	6
3NCD	6
3CD	7
4NCD	8
4CD	12

Table 2b: Number of NP samples in every

Group	Number of AF samples
1NCD NH	10
1 NCD H	0
2NCD NH	7
2 NCD H	0
2CD NH	3
2 CD H	4
3NCD NH	5
3 NCD H	1
3CD NH	1
3CD H	5
4NCD NH	4
4NCD H	6
4 CD NH	1
4CD H	4

Table 3a: number of AF samples in every group

Group	Number of NP samples
1NCD NH	9
1 NCD H	0
2NCD NH	4
2 NCD H	3
2CD H	6
2CD NH	0
3NCD NH	4
3NCD H	2
3 CD NH	1
3 CD H	6
4NCD NH	5
4 NCD H	3
4CD NH	0
4CD H	12

Table 3b: number of NP samples in every group

PGE2 measurements

Eppendorf tubes were filled with 400µl and 750µl of Roche complete Lysis-M EDTA-free buffer to lysate NP and AF samples, respectively. All samples were weighed on a Mettler Toledo balance type AB204 and subsequently cut into small pieces with sterile scissors. After cutting each sample, the scissor was disinfected with milliQ and 70% ETOH. Sterile stainless steel beads were added to each Eppendorf tube with sterile forceps and then the tissues were lysed in a Qiagen TissueLyser type II during 2 minutes with a frequency of 20Hz. Afterwards, the beads were removed by using a magnet. The samples were then centrifuged for 15 minutes in a Eppendorf Centrifuge type 5415R with maximum frequency. The amount of supernatant was measured by pipetting it into new Eppendorf tubes. The supernatants and the pellets were stored at -80ºC (attachment 1). To measure the PGE2 content in the supernatants, the PGE2 high sensitivity EIA kit (Enzo) was used. The supernatants were thawed and some samples were diluted. The assay was performed according to the manual (attachment 5). However, because the samples were stored in a Roche Lysis buffer, the standard curve was prepared in Roche Lysis buffer. Samples were measured in mono and if PGE2 levels were higher than the highest standard, samples were diluted. After incubating the plate, 300µL of wash solution was used and the washing was repeated 5 times. Absorbance data were generated with a DTX 880 Multimode Detector at 405 nm. Biorad plate reader software (Microplate Manager™ 6, Version 6.3) was used for analysis of absorbance data. The PGE2 content of the samples was normalized by DNA, weight and protein content of the samples.

COX2 measurements

For measuring the COX-2 protein expression, histological sections from the study of Bergknut et al(N. Bergknut et al., 2013) were used. In this study, the thoracolumbar and lumbosacral vertebral columns (T11-S1) of 15 randomly selected fresh (<12 h of death) canine cadavers were collected. Various dog breeds (both chondrodystrophic and nonchondrodystrophic), ages, and gender were included. The samples were collected from five Beagles (five chondrodystrophic dogs), three Foxhounds, three Kerry Beagles, one Welsh Terrier, and three mixed-breed dogs (10 non-chondrodystrophic dogs). The dogs (10 females, 5 males) ranged from 1 to 16 years of age (median age, 5 years) and weighed between 9 and 44 kg. Materials were collected from laboratory dogs that had been euthanized in an unrelated study or from client-owned dogs (permission to use the spine was granted by the owners) that were submitted for necropsy to the Department of Pathobiology at the Faculty of Veterinary Medicine, Utrecht University. None of the dogs had a reported history of back problems. After dissection, the spines were transected in the midsagittal plane using a belt saw. High-resolution photographs were taken of the midsagittal surface of each spinal unit (endplate-intervertebral disc-endplate) and were used for grading according to the Thompson scheme. Fresh nucleus pulposus tissue from one half of each IVD was snap frozen for glycosaminoglycan (GAG) analysis. Due to the cutting procedure there was only enough NP material to perform a GAG assay on 118/150 IVDs and these were the only IVDs included in this study. The remaining half of each IVD was retained for histological examination. Midsagittal slices (3– 4 mm thick) were cut and the 118 intervertebral segments were fixed in 4% neutral buffered formaldehyde solution and subsequently decalcified in EDTA. After decalcification, all samples were embedded in paraffin and sliced with a microtome. All 118 IVD samples were classified according to the grading scheme by Thompson et al. (1990). Seven histological samples per Thompson grade (grades I, II, III, IV, and V), i.e. 35 samples in total, were randomly selected for histological evaluation(N. Bergknut et al., 2013).

Those 35 patient samples were stored at 4ºC. Before dehydration of the paraffin sections, the slides were heated with a Grant UBD2 Heating Block up to 65ºC. The staining was performed according to the protocol (see attachment 3). A COX-2 Monoclonal Antibody was used (isotope IgG1 and a mouse as host, see attachment 4). Immunohistochemical evaluation was performed by observing the sections under a light microscope. Positive staining with COX-2 was defined as brown staining in the cytoplasm or nuclei.

GAGs measurements

The dimethylmethylene blue assay (DMMB assay/Farndale assay) was used to measure the sulfated GAG content of the NP and AF tissue of all 106 samples (attachment 1,2). The sulfated GAG content was measured in the pellets as well as in the supernatants. The pellets were stored at -80ºC. Protein digestion of the pellets was performed overnight at 60°C in a papain digestion solution, using a Mini-Hybridisation Oven OV2. The Eppendorf tubes that contain NP tissue were filled with the volume of the supernatant plus 100 µL papain buffer. The tubes that contain AF were filled with the volume of the supernatant plus 250 µL papain buffer. After incubation, the samples were centrifuged in an Eppendorf Centrifuge type 5414R and they were incubated for an additional hour at 60°C. The DMMB assay was executed according to the protocol (attachment 2). Samples were diluted in PBS-EDTA (1:50; 1:100; 1:1000 or 1:1001).The plate was read at wavelengths of 540 nm and 595 nm using a Beckman Coulter Multimode detector DTX 880. After finishing the assay, the pellets with papain digestion solution were stored at -80ºC and the diluted samples were stored in -20 ºC.

To measure the sulfated GAG content in both NP and AF supernatants, they were diluted 1:10 with papain digestion solution. The samples were incubated overnight at 60°C, using a Mini-Hybridisation Oven OV2. After incubation, the supernatants were centrifuged with a Hettig Zentrifugen centrifuge type EBA 12. The supernatants were then diluted in PBS-EDTA 1:10 or 1:30. After finishing the assay, the supernatants were stored at -20ºC and the diluted supernatants were stored at 4°C. The amount of GAG was calculated in Excel by use of the polynomic formula y=ax2+bx+c. The GAG content of the samples was normalized by the weight and the DNA content of the samples.

DNA content

The DNA content of all the 106 IVD samples was measured in the digested pellets, using a Qubit 2.0 fluorometer (Invitrogen) and its corresponding dsDNA BR Assay Kit. The assay was performed according to the manual (attachment 6). Samples were diluted 1:40 in Qubit working solution. DNA content was normalized for weight to obtain information on the cellularity of samples.

Protein content

The protein content was measured in the supernatants of the NP tissue samples, using the DC Protein Assay from BioRad Laboratories (see for the protocol attachment 7). 7 dilutions of BSA protein standard were prepared, from 0.2 mg/ml to 1.5 mg/ml, as follows:

1. 50 µl stock BSA plus 450 µl PBS	1.50 mg/ml
2. 67 µl 1 plus 33 µl PBS	1.00 mg/ml
3. 50 µl 1 plus 50 µl PBS	0.75 mg/ml
4. 33 µl 1 plus 67 µl PBS	0.50 mg/ml
5. 17 µl 1 plus 83 µl PBS	0.25 mg/ml
6. 8,5 µl 1 plus 91,5 µl PBS	0.125 mg/ml
7. 4,25 µl 1 plus 95,75 µl PBS	0.0625 mg/ml
8. 0 µl1 plus 100 µl PBS	0.00 mg/ml

The supernatants of the NP tissue samples were diluted (1:19 and 1:10) prior to measurements. 5 µl of the standards and samples were pipetted in a clean and dry microtiterplate. The standards were pipetted in duplicate, the samples in mono. After adding Reagentia A* and B into each well, absorbance was read at 650nm using a DTX 880 Multimode Detector. The total protein content in each sample was then calculated in Excel by using the extinction results and the linear formula y=ax+b.

Statistical analysis

For statistical analysis, the Software R (Version) was used. To perform the statistical analysis, the samples in our dataset were classified in a different way. Of each sample was reported whether herniation, protrusion or no displacement of the NP towards the AF was observed. A multiple linear regression model was used to fit log-transformed data; normal distribution was verified. The dependent variable in this linear regression model was PGE2/DNA or PGE2/weight. The explanatory variables are CD/NCD and the degree of displacement (hernia, protrusion or no displacement). Because of small group sizes, Pfirrmann scores (grade 1-4) could not be added as an explanatory variable in this multiple linear regression model. The statistical analysis of this classification of our dataset was beyond the scope of this research report and therefore results are described for the classification into Pfirrmann scores and type of dog breed.

Results

This result section will start with reviewing the results of the NP tissue, followed by the results of the AF tissue. For both NP and AF, first the primary readout parameter will be discussed, followed by the secondary parameters. This section will end with a review of the COX2 measurements.

Results NP samples

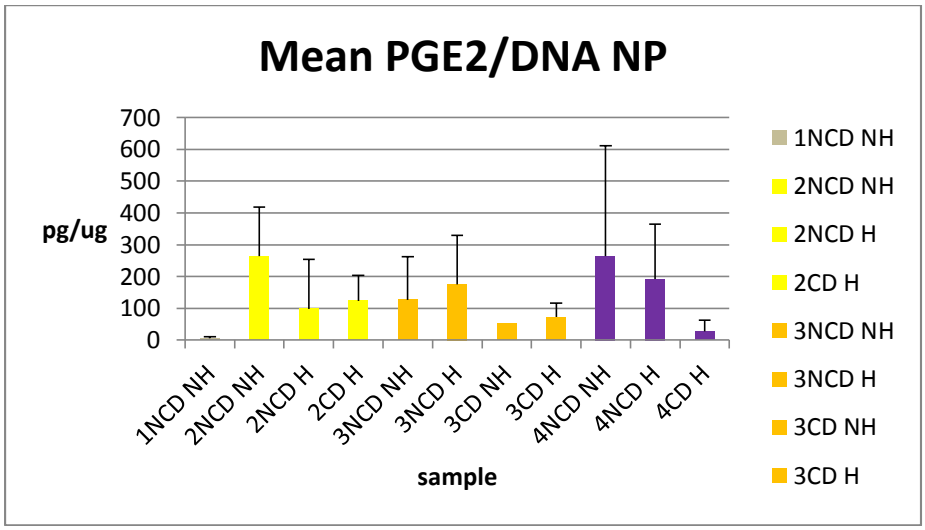

Figure 21: Mean PGE2/DNA in the nucleus pulposus

Figure 21 shows that herniated NP samples of NCD dogs have a lower PGE2/DNA ratio compared with non-herniated NP samples of NCD dogs. This can be seen at different stages of degeneration (groups with Pfirmann score 2 and 4). Furthermore, this figure shows that the 1NCD NH samples have a lower PGE2/DNA ratio compared with the higher NCD degeneration grades.

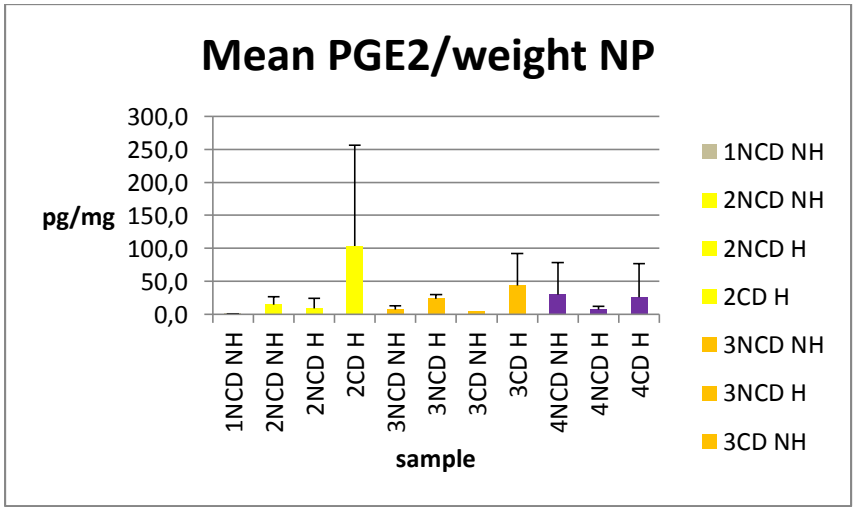

Figure 22: Mean PGE2/weight in the nucleus pulposus

Figure 22 shows that herniated NP samples of CD dogs, contain more PGE2 than herniated NP samples of NCD dogs. This can be seen at different stages of degeneration (groups with Pfirmann score 2,3 and 4).

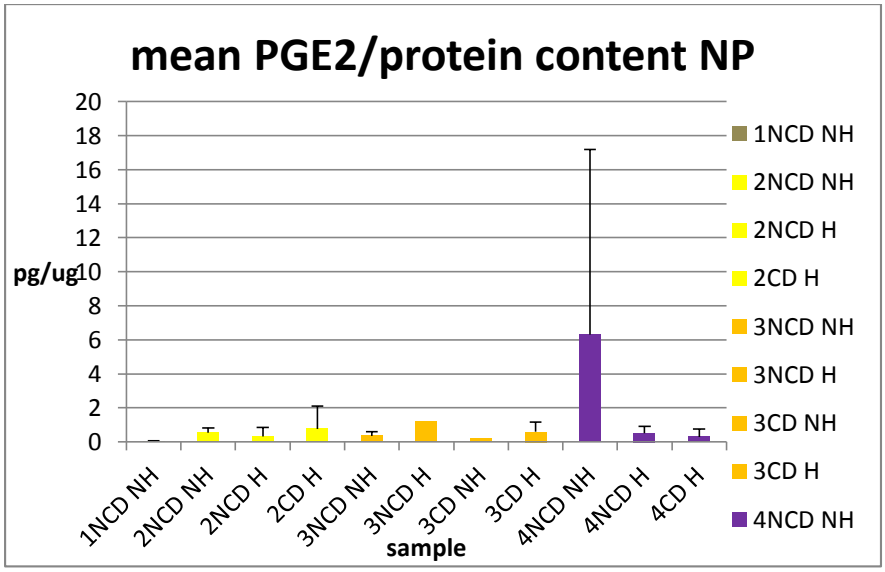

Figure 23: Mean PGE2/protein content in the nucleus pulposus

Figure 23 shows similar PGE2/protein levels in all groups, except for the herniated samples of 4 NCD dogs, that also show a very high standard deviation.

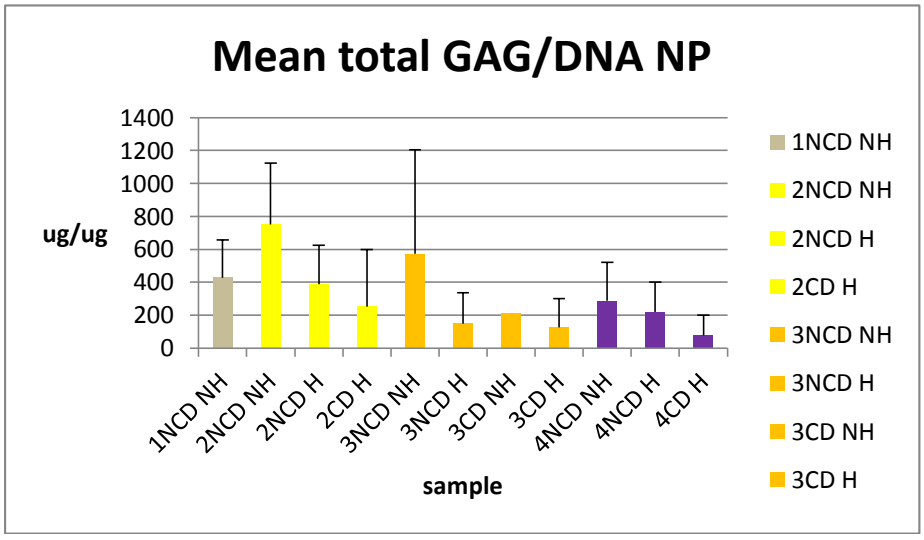

Figure 24: Mean total GAG/DNA in the nucleus pulposus

Figure 24 shows that herniated NP samples have a lower GAG/DNA ratio compared with non-herniated NP samples. This can be seen in the following groups: 2NCD NH compared with 2NCD H, 3NCD NH compared with 3NCD H, 3CD NH compared with 3CD H and 4NCD NH compared with 4NCD H.
Furthermore, a decrease of the GAG/DNA ratio can be observed as degeneration increases. This can be seen in the following groups: 2NCD NH - 3NCD NH – 4NCD NH and 2CD H - 3CD H - 4 CD H.

Furthermore, figure 24 shows that CD tissue has a lower GAG/DNA ratio compared with NCD tissue. This can be seen for all the different groups.

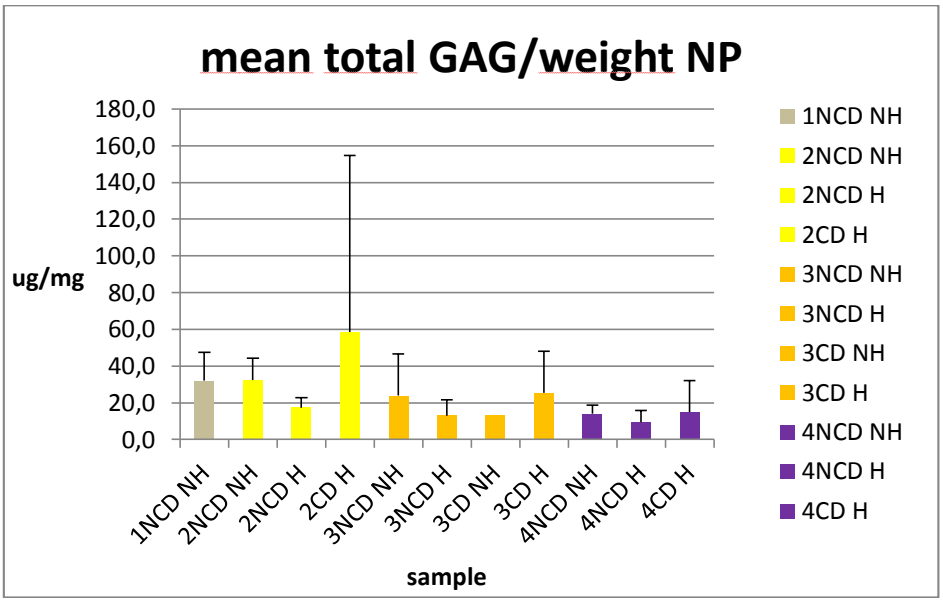

Figure 25: Mean total GAG/weight in the nucleus pulposus

Figure 25 shows that the total GAG content in herniated samples of chondrodystrophic dogs is higher compared with herniated samples of non-chondrodystrophic dogs. This can be seen at different stages of degeneration (groups with Pfirrmann score 2,3 and 4). Furthermore, this figure shows that a decrease in GAG/weight ratio can be observed as degeneration increases.

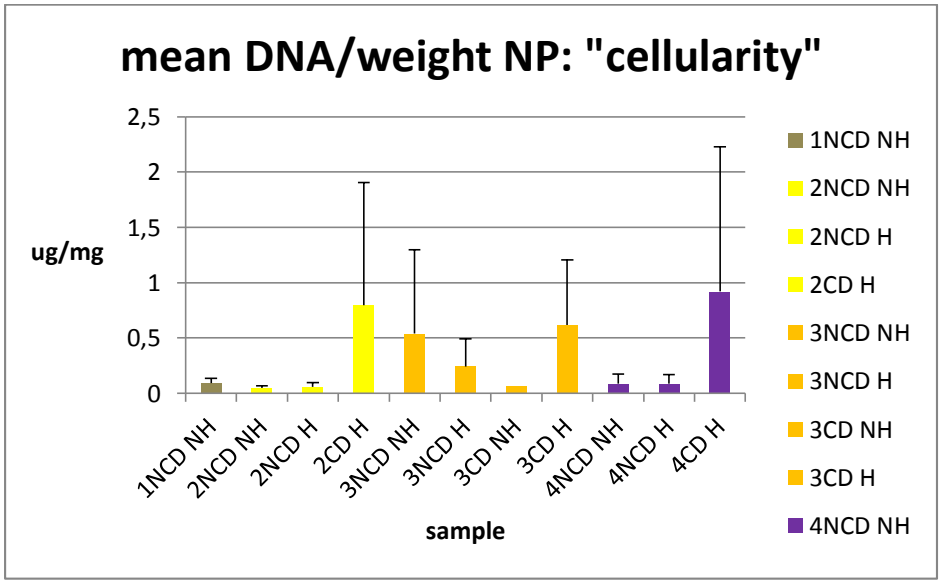

Figure 26: mean DNA/weight in the nucleus pulposus, to obtain an idea about the cellularity of the samples

To obtain information on the cellularity of the samples, DNA/weight was evaluated. Figure 26 shows that the DNA content in herniated NP tissue of chondrodystrophic dogs is higher in comparison with the DNA content in herniated NP samples of non-chondrodystrophic dogs. This can be seen at different stages of degeneration (groups with Pfirmann score 2, 3 and 4).

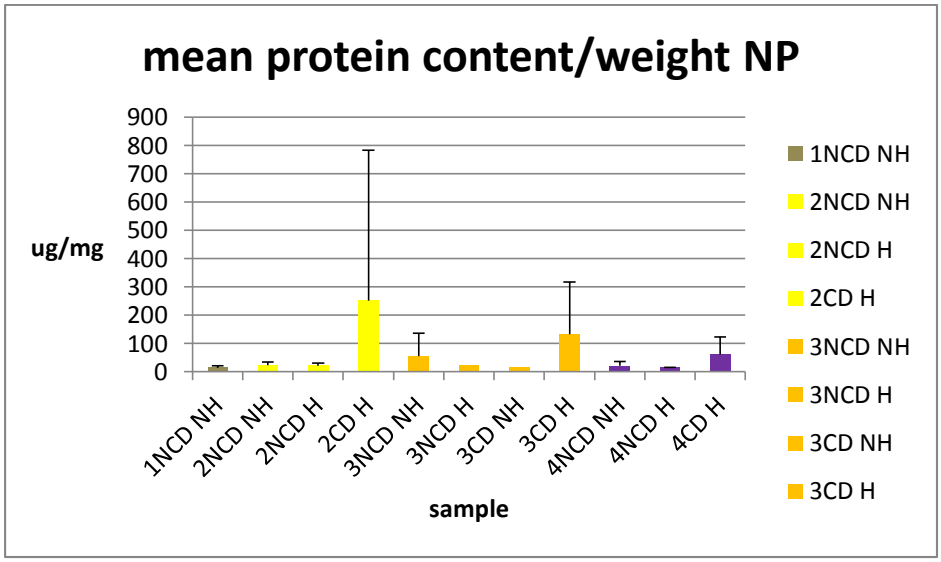

Figure 27: mean protein content/weight in the nucleus pulposus

Figure 27 shows that the protein content/weight in herniated NP tissue of chondrodystrophic dogs is higher in comparison with the protein content/weight in herniated NP samples of non-chondrodystrophic dogs. This can be seen at different stages of degeneration (groups with Pfirmann score 2,3 and 4).

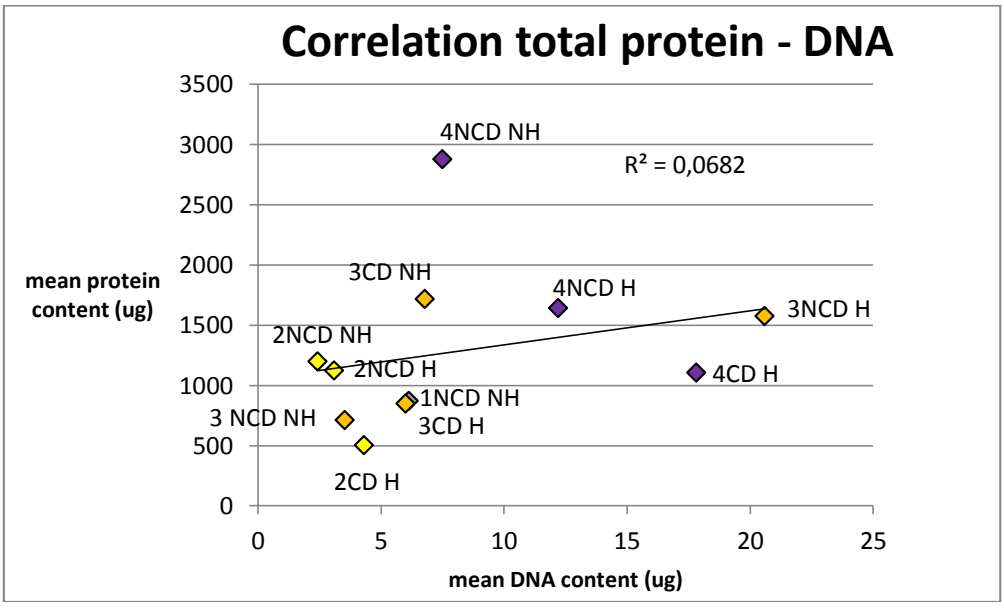

Figure 28: Correlation between total protein and DNA in the nucleus pulposus

Figure 28 shows a correlation coefficient of 0.0682 between protein content and DNA content.

Results AF samples

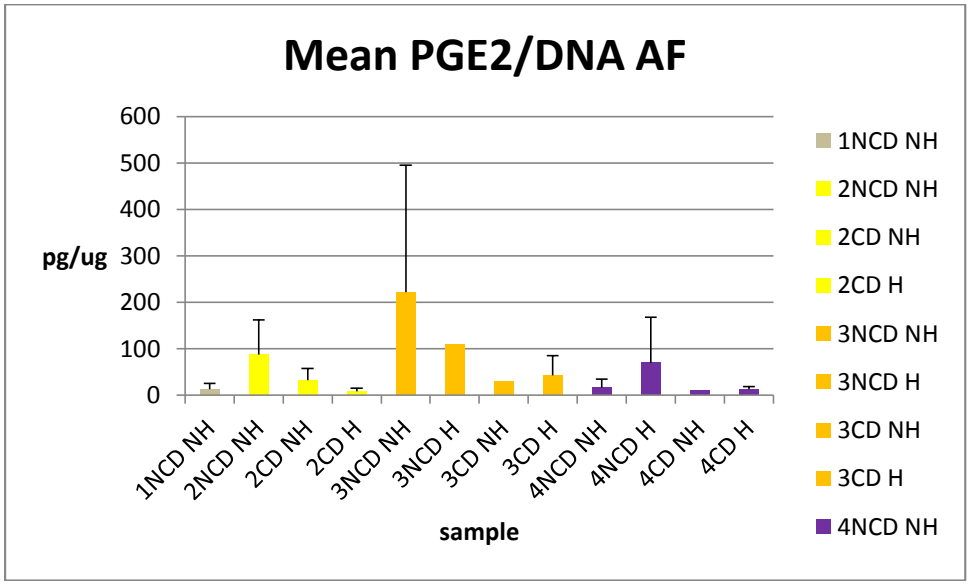

Figure 29: Mean PGE2/DNA in the annulus fibrosus

Figure 29 and 30 show that in the AF the herniated samples of CD dogs have lower PGE2/DNA (fig. 29) or PGE2/weight (fig. 30) contents than the herniated samples of NCD dogs. Furthermore, the PGE2 content of the 1NCD group is higher in proportion to the other groups, than the PGE2 content of the 1NCD group in the NP. The PGE2 contents of group 2CDH, 3CDH, 4CDH and 4NCD NH are higher in the NP than in the AF. The PGE2 content in group 4 is lower than in group 1,2 and 3, except for group 4NCD H but this group has a very high standard deviation.

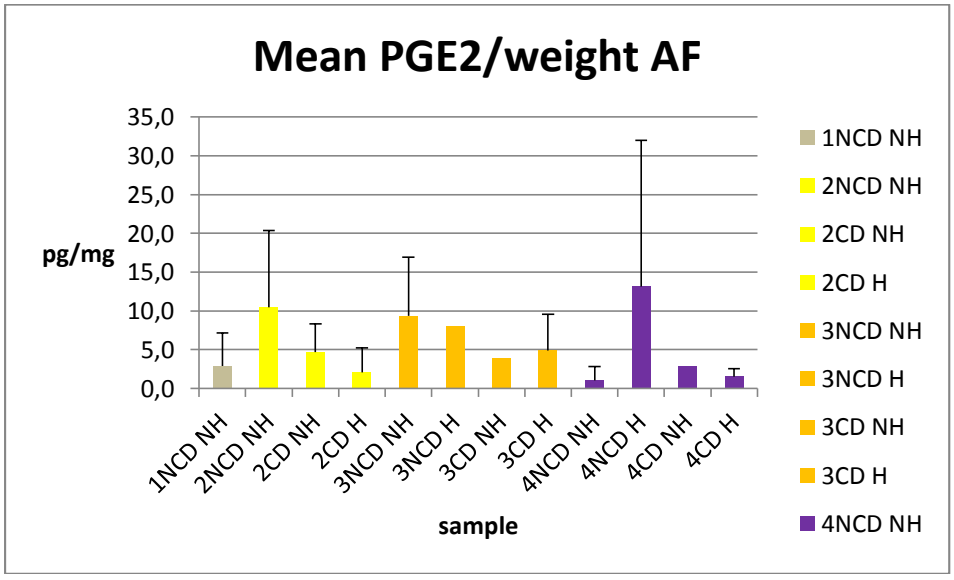

Figure 30: Mean PGE2/weight in the annulus fibrosus

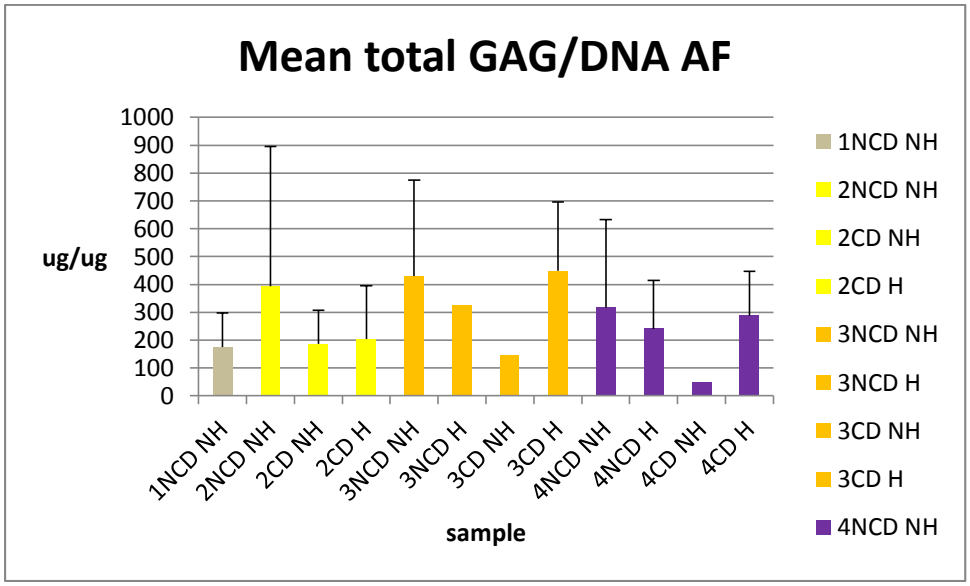

Figure 31: Mean total GAG/DNA in the annulus fibrosus

Figure 31 shows that in CD NH tissue GAG/DNA levels decrease with degeneration.

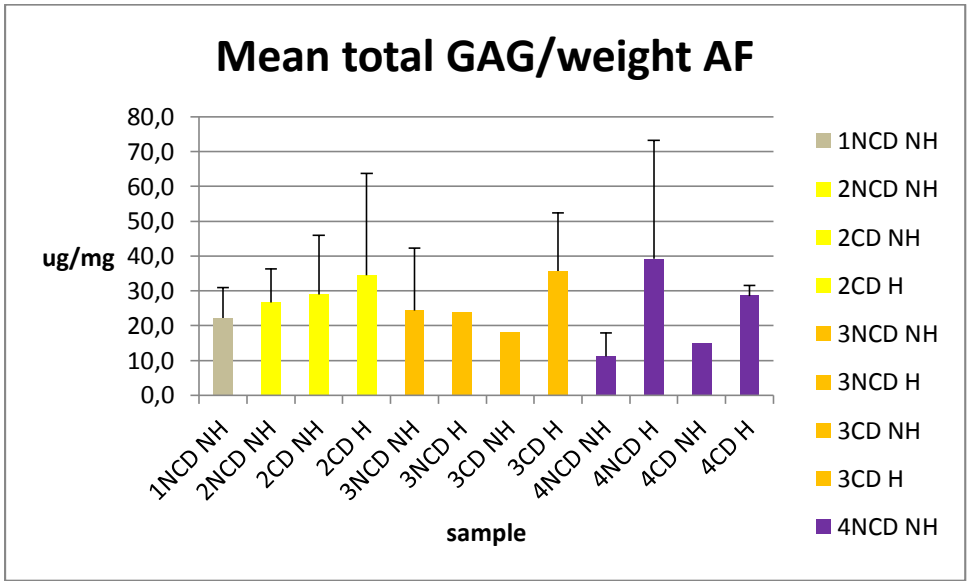

Figure 32: Mean total GAG/weight in the annulus fibrosus

Figure 32 shows that in early stages of degeneration, CD dogs have a higher GAG/weight content than NCD dogs (this can be seen in group 2 and in group 3 for the herniated samples). Furthermore, herniated samples have a higher GAG content than non-herniated samples. This can be seen in every group except for the 3NCD group.

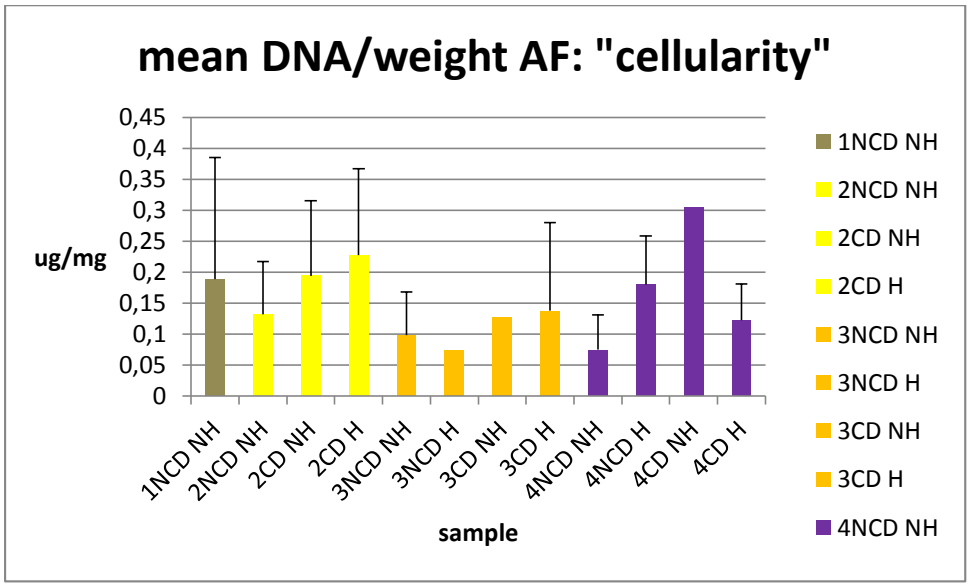

Figure 33: Mean DNA/weight in the annulus fibrosus, to obtain an idea about the cellularity of the samples

Figure 33 shows that DNA/weight in NCD NH tissue decreases with degeneration. This trend is also seen in CD H tissue.

Results COX2 measurements

Immunohistochemical evaluation was performed by observing the sections under a light microscope. Positive staining with COX-2 was defined as brown staining in the cytoplasm or nuclei. Antigen expression could be quantified on the basis of staining intensity and the proportion of positively stained cells. Only very slight staining was observed. The staining intensity was too low (some very pale brown-colored cells were seen) to label cells with certainty as positive for COX-2 expression. Furthermore, a lot of brownish background was seen that complicated the evaluation of COX-2 expression.

Discussion

Nucleus Pulposus

The finding that herniated NP samples of NCD dogs have a lower PGE2/DNA ratio compared with non-herniated NP samples of NCD dogs (fig 21), can be explained by the fact that herniation leads to an inflammation reaction. Inflammatory cells increase the DNA content of the sample. Because of this increased DNA content in herniated samples, the PGE/DNA ratio in those samples decreases. Non-herniated samples contain less inflammatory cells and therefore the DNA content in those samples is lower. The lower PGE2/DNA ratio in herniated samples indicates, that despite higher cellularity, the amount of PGE2 is produced only by a subpopulation of cells.

The finding that herniated NP samples of CD dogs have a higher PGE2/weight ratio than herniated samples of NCD dogs (figure 22), can be explained by the fact that CD dogs generally suffer from type I herniation. Because of the acute onset of this type of herniation, a higher PGE2 content can be found in the NP tissue from CD dogs in comparison with NP

tissue from NCD dogs who generally suffer from the more chronic type II herniation(Hazewinkel et al., 2013; Kranenburg et al., 2013). This finding is comparable to the results of a study in which they investigated PGE2 content in herniated lumbar disc disease in humans. Higher PGE2 levels were found in extruded NP samples than in protruded NP samples(O'Donnell & O'Donnell, 1996).

The 1NCD NH group in our study did not consist of patient material. Interestingly, the PGE2 content of this group was much lower compared to the other groups which consisted of samples of dogs that showed clinical signs(figure 21 and 22). It seems that the lack of clinical signs is associated with a lower PGE2 content. The study of Van Dijk et al. included human intervertebral disc tissue coming from autopsy subjects that died of myocardial infarction and carcinomas. The disc degeneration in those persons did not cause pain(van Dijk et al., 2014). The lower PGE2 levels found in those samples originating from humans without clinical signs, together with the higher PGE2 levels that we found in samples coming from dogs with clinical signs, may indicate that the presence of clinical signs is associated with elevated PGE2 levels. In 1996 Kang et al. performed a study to determine whether tissue from human herniated lumbar discs was producing biochemical agents that might play a significant role in disc herniation and in the pathophysiology of lumbar radiculopathy. Disc specimens were obtained from adult patients that underwent surgery for persistent radicular symptoms. The control group consisted of lumbar intervertebral discs collected from patients with scoliosis or traumatic burst fracture, who did not have a history of radiculopathy or low back pain. In this study the PGE2 content was significantly higher in the herniated disc tissue compared with the control discs(Kang et al., 1996). O'Donnell performed a study to investigate the content of PGE2 in human lumbar disc herniations in relation to clinical and anatomical findings. The results of that study suggest a role for PGE2 in the mediation of some of the manifestations of disc herniation, especially the symptom of radiating distress(O'Donnell & O'Donnell, 1996). All those results may indicate an association between elevated PGE2 levels and clinical signs. The finding that the PGE2/protein content ratio of herniated NP samples of CD dogs is low (figure 23), is also in accordance with the theory that CD dogs generally suffer from the acute Hansen type I herniation. In herniated IVD material, the expression of the inflammatory mediators interleukin (IL)-1, tumor necrosis factor (TNF)-α, prostaglandin E2, and nitric oxide (NO) is increased. The expression of various matrix metalloproteinases (MMPs) is up-regulated. Inflammatory mediators, growth factors and enzymes are also a substantial part of the total protein content. Due to all those changes the total protein content increases, especially in herniated discs of CD dogs because of the acute inflammatory reaction. Therefore, in those samples the protein content/weight ratio gets higher (figure 27). However, those herniated CD samples also showed an increased PGE2 content (figure 22). If the PGE2 content increases, but so does the protein content, the PGE2/protein ratio remains low. In this way PGE2 levels may be underestimated. From those observations we conclude that for this study, the PGE2/protein content ratio is not a reliable measure to represent PGE2 contents.

As compared to the study performed by Van Dijk et al, we detected higher PGE2/protein levels (figure 23). We compared our levels with their measured levels at day 0. Their study was an in vitro study, and cells under those conditions spontaneously produce inflammatory mediators. Because at day 0 there was not much time to produce inflammatory mediators, we decided these measures would be the best comparison. Van Dijk et al. reported that the measured PGE2 levels probably were basal levels which were the result of COX1 activity (van Dijk et al., 2014). We detected higher PGE2 levels, which could mean that these PGE2 levels represent elevated levels and are the result of COX2 activity. As depictured before, the PGE2 content of the 1NCD NH group in our study, which did not consist of patient material,

showed a much lower PGE2 content compared to samples of dogs that showed clinical signs(figure 21 and 22). Those lower PGE2 contents may be the result of COX1 activity.

The observation that herniated NP samples have a lower GAG/DNA ratio compared with non-herniated NP samples (figure 24), can be explained as following: the healthy NP is relatively densely populated by notochordal cells that synthesize and remodel the matrix. This matrix consists of negatively charged proteoglycans interwoven in a mesh of collagen fibers. The proteoglycan molecules consist of a protein backbone with negatively charged glycosaminoglycan (GAG) side chains(P. N. Bergknut, 2011). So in fact, the GAGs are synthesized by the cells of the NP. Hansen type I herniated samples contain more cells because of incoming inflammatory cells. Those cells are not able to synthesize GAG molecules. In case of a hernia, the total GAG/DNA ratio decreases, because cellularity increases and therefore DNA content increases. In CD tissue the GAG/DNA levels are lower compared to those levels in NCD tissue. This finding is consistent with the fact that in CD dogs, notochordal cells disappear at a very young age, while in NCD dogs the notochordal cells remain the prominent cell type during the majority of life. The reduced presence of notochordal cells in CD dogs means less production of GAG molecules. The decrease in GAG/DNA ratio that can be seen in CD dogs as degeneration increases, can be explained by the fact that more degenerated NPs contain less notochordal cells and thus less GAG molecules are produced(P. N. Bergknut, 2011).

The finding that the total GAG/weight content in herniated NP samples of chondrodystrophic dogs is higher than those in non-chondrodystrophic dogs (figure 25), can be explained by the acute onset of signs in chondrodystrophic dogs versus the chronic appearance in non-chondrodystrophic dogs. If the problem is a chronic one, like it generally is in NCD dogs, increased degradation of GAG molecules will result in a decreased GAG content. In CD dogs, because of the acute onset less degradation took place. Bergknut et al. reported that in dogs, the mean GAG concentrations in the NP are negatively correlated with increasing degeneration(N. Bergknut et al., 2012). Therefore, in our study we expected to see a decrease in GAG content as degeneration increases. This is indeed what we observed.
As compared to the results of Bergknut et al., we found higher GAG/weight ratios. To measure the sulfated GAG content, Bergknut used 123 canine NP samples. Those samples originated from dogs without a history of IVDD-related diseases (N. Bergknut et al., 2012). The samples in our study originated from dogs suffering from IVD-related diseases. Furthermore, we made a subdivision in NCD and CD dogs, as well as herniation or no herniation. The 123 samples that Bergknut used in his study originated from a mixed population of CD and NCD dogs. Therefore, no subdivision could be made between NCD and CD samples and moreover, no subdivision was made between herniated and non-herniated samples. At last, the collecting and processing of the samples differed in both studies. All those differences may be responsible for the dissimilar GAG/weight ratios that we found between the studies.

The observed phenomenon that the DNA/weight ratio in herniated NP samples of chondrodystrophic dogs are higher than those of non-chondrodystrophic dogs (figure 26), can be explained by the differences in cellularity of the samples. In case of a Hansen type 1 IVD herniaton, an acute inflammatory reaction is evoked when disc material herniates into the spinal canal. Inflammatory cells such as lymphocytes, neutrophils and macrophages can be found in extruded disc material(Kranenburg et al., 2013; Royal et al., 2009). Furthermore, hemorrhage and neovascularization can occur. In case of a type 2 IVD herniation, blood vessels may grow into the periphery of the disc, leading to inflammatory changes within the

AF. Lymphocytes, plasma cells, macrophages and granulation tissue can be found in the intervertebral disc. In contrast to a type I hernia, a type 2 herniation reflects a more chronic inflammatory reaction with signs of tissue repair. Nuclear material can be resorbed which causes the inflammation reaction to settle down(Hazewinkel et al., 2013). It is reported that type 1 hernias occur mainly in CD dog breeds, whereas type 2 IVD herniations occur predominantly in NCD dogs(Brisson, 2010; Royal et al., 2009). In CD dogs, herniation is acute and acute inflammation leads to a lot of inflammation cells. Those inflammation cells lead to a higher DNA content in the nucleus pulposus. Inflammation cells do not really contribute to the weight of the samples, because the weight of the samples is especially influenced by the matrix surrounding the cells. Therefore the DNA/weight ratio in those herniated CD samples gets high. IVD degeneration in NCD dogs has a more chronic appearance. Less inflammation cells are present, and so the DNA content in herniated NCD samples is lower. Therefore the DNA/weight ratio gets lower.

The differences in DNA/weight ratio between the samples (figure 26), also explain the different pattern that can be observed between the PGE2/DNA (figure 21) and the PGE2/weight graph (figure 22). The differences in cellularity lead to dissimilarities between the PGE/DNA and the PGE2/weight graph. This makes clear that it does matter whether the DNA content or the weight of the samples is used as a correction factor for the PGE2 content. We preferred to use the weight of the samples as a correction factor. Inflammation could increase the cellularity of the samples and DNA as a correction factor may therefore underestimate the PGE2 content. Furthermore, the DNA content of the samples was only measured in the pellets. The weight of the samples was determined before they were further processed, so in contrast to the DNA content, the weight represents the intact sample.

The finding that the protein content/weight ratio in herniated samples of chondrodystrophic dogs is higher than the protein content/weight ratio in herniated samples of non-chondrodystrophic dogs (figure 27), can again be explained by the fact that chondrodystrophic dogs generally show herniation type I which has a sudden onset and an explosive character. An acute inflammation reaction occurs and inflammatory mediators are expressed. In herniated IVD material, the expression of the inflammatory mediators interleukin (IL)-1, tumor necrosis factor (TNF)-α, prostaglandin E2, and nitric oxide (NO) is increased.(Kang, Stefanovic-Racic, McIntyre, Georgescu, & Evans, 1997). Furthermore, increased concentrations of growth factors, such as TGF, have been reported in degenerated intervertebral discs. It is thought that those growth factors attempt to increase matrix synthesis and repair. The process of remodeling and breakdown of the extracellular matrix in the IVD is regulated by enzymes, such as matrix metalloproteinases (MMPs) which are produced by the cells of the IVD(P. N. Bergknut, 2011). In degenerated intervertebral discs, changes in the expression of mediators of matrix degradation and remodeling occur. The expression of various matrix metalloproteinases (MMPs) is up-regulated(Hazewinkel et al., 2013). Due to all those changes the total protein content increases, especially in herniated discs of CD dogs because of the acute inflammatory reaction.

The finding that protein content is not correlated to DNA content (figure 28), reveals that the total protein content is not only influenced by the amount of cells, but that other components are of influence as well.

Annulus fibrosus

In contrast to the NP samples (fig. 22), herniated AF samples of CD dogs have lower PGE2/DNA ratios (fig. 29) and PGE2/weight ratios (fig. 30) than herniated samples of NCD dogs. This contradiction can be explained as follows: CD dogs generally suffer from type I herniation which has an acute onset. In type I herniation, the NP passes the AF very quickly. The AF is exposed to inflammatory mediators only for a short period of time. NCD dogs mostly suffer from herniation type II, which is a more gradual process. The nucleus pulposus will slowly protrude into the annulus fibrosis and so the annulus fibrosis will be exposed to inflammatory mediators for a longer period of time. Therefore, higher PGE2 contents can be found in AF samples of NCD dogs than in AF samples of CD dogs. In case of acute herniation (Hansen herniation type I), the nucleus pulposus is suddenly exposed to a different environment and therefore many inflammatory mediators will be present. In the more chronic situation of herniation type II, the nucleus pulposus is slowly exposed to a different environment and inflammatory mediators. Because of this gradual process, less PGE2 will be found within the NP tissue. Therefore, higher PGE2/weight ratios can be found in NP samples of CD dogs.

The finding that the PGE2 content in the NP is higher than in the AF (figure 22 and 30), can be explained by the fact that the problem of degeneration starts within the center of the IVD. The first alterations that can be noticed in IVD degeneration are the cellular changes within the nucleus pulposus. The NP is exposed to more inflammatory stimuli and therefore the PGE2 content in the NP samples is higher.

Herniated samples of CD dogs have lower PGE2/DNA ratios (figure 29) and PGE2/weight ratios (figure 30) than herniated samples of NCD dogs. Herniation in NCD dogs is a more gradual process than it is in CD dogs. Therefore, the AF in NCD dogs might be exposed to inflammatory mediators for a longer period of time. In CD dogs, during acute herniation the NP tissue extrudes trough the AF in a sudden and explosive way. The difference in exposure time to inflammatory mediators may be responsible for the differences in PGE2 content.

The PGE2/weight ratio of the 1NCD group in the AF is higher in proportion with the other groups (figure 29 and 30), than the PGE2/weight content of the 1NCD group in the NP (figure 26). This might be due to differences in tissue type between NP and AF tissue. Obviously, the basal PGE2 production in those two tissue types differs from each other. Differences in tissue type between the NP and AF were earlier reported by Miyamoto et al. In their study they investigated the involvement of cyclic mechanical stress in the production of inflammatory agents by disc cells. Doses of PGE2 were measured in culture supernatants. Annulus fibrosus cells showed a stronger reactivity to mechanical stress and inflammatory stimuli than nucleus pulposus cells(Miyamoto et al., 2006).

The finding that the PGE2/weight ratio in group 4 is lower than in group 1,2 and 3 (figure 30), indicates that in this stage of degeneration, less PGE2 is present. This can be due to less PGE2 production per cell, but it is more likely that the PGE2 is produced by less cells or by only a subpopulation of cells. It is known that in chronic processes, cells may be substituted by other tissue. Granulation tissue may arise, which does not produce PGE2. Arising granulation tissue also accounts for the decreasing DNA/weight ratio that we observed in NCD NH and CD H tissue (figure 33). Granulation tissue does not contain many cells, so the DNA content of those samples decreases as granulation tissue arises. At the same time the weight of the samples increases, as granulation tissue has a positive influence on the weight of the samples. Therefore, the DNA/weight ratio decreases.

We did not look at what kind of medicines the patients in our study received prior to surgery, but that could have influenced PGE2 levels. PGE2 belongs to the class of prostanoids, which are produced by cyclooxygenase-1 and 2 (COX 1 and COX2). Most nonsteroidal anti-inflammatory drugs (NSAIDs) used in veterinary practice are aimed at shutting down COX2. Therefore administration of NSAIDs, specifically in IVDs with chronic inflammation and thus blood vessel ingrowth, may have had an effect on the PGE2 content. Glucocorticoids have an influence at the top of the inflammatory cascade(Ayroldi et al., 2012). Glucocorticoids are steroidal anti-inflammatory drugs which inhibit nuclear transcription processes. Therefore, glucocorticoids shut down the whole cascade. As a result, PGE2 levels can also be influenced by administration of glucocorticoids. However, because the working mechanism of NSAIDs and glucocorticoids differs, the degree in which COX isoforms and PGE2 are inhibited, may vary. Administration of different medicines prior to surgery could provide an explanation for differences we found in PGE2 content between the patient samples. Glucocorticoid administration appeared to have a negative effect on dogs with medically treated disc herniation, in contrast to administration of NSAIDs. This difference may show that, although both medicines are aimed at knocking down the inflammatory cascade, results between different kind of medicines can differ(Levine et al., 2007b).

The graph which represents the GAG/DNA ratios in the AF (figure 31), shows that in CD NH tissue GAG/DNA levels decrease with degeneration. As depicted in the mean DNA/weight graph of the AF (fig.33) the DNA/weight ratio in CD NH tissue remains approximately the same. Obviously, the mean total GAG concentration decreases with degeneration. A decreasing mean total GAG concentration in combination with a stabile cellularity, will result in a lower mean total GAG/DNA ratio. However, this is not what we expected. It is generally assumed that the GAG concentration in the AF increases with degeneration, so we expected to find higher GAG contents as degeneration increases. This contradiction between what we observed and what we expected may be explained by the very high standard deviations and low group sizes.

The observation that in early stages of degeneration, CD dogs have a higher GAG content than NCD dogs (figure 32), indicates that IVD degeneration might develop in a different way in CD and NCD dogs. In CD dogs, it might be that the AF becomes weaker, which would also explain why type I herniation occurs more often. Weakening of the AF is associated with higher GAG content in the AF, because GAGs are produced by chondrocyte-like cells which increase in amount as degeneration increases(P. N. Bergknut, 2011; Hazewinkel et al., 2013). At the same time, this finding shows the disadvantages of the use of the Pfirmann grading system to determine the stage of degeneration of the intervertebral disc. The Pfirmann grading system only takes into account the water content of the NP and it does not evaluate the structure of the AF(P. N. Bergknut, 2011; Pfirrmann et al., 2001). With the use of this system, different intervertebral discs might be classified as the same stage of degeneration, although degeneration in the AF might be much further in one sample compared to the other. Besides, we found that herniated samples have a higher GAG content in the AF than non-herniated samples (figure 32). Again, this can be explained by the fact that herniation is a result of weakening of the AF(P. N. Bergknut, 2011; Hazewinkel et al., 2013). Because of ruptured AF fibers, herniation can occur. A higher GAG content in the AF is caused by the presence of more chondrocyte-like cells, so the degeneration process in those samples is in a further stage. Thence the AF is weakened more and this in turn increases the chance to herniate.
Based on the assumption that the GAG content in the AF increases with degeneration, we expected to find an increase in GAG/weight content in the AF as degeneration increases. However, this cannot be observed from our dataset (figure 32). An explanation for the fact

that this positive correlation can't be observed from our dataset, is that the AF in our samples may be degenerated to a lesser extent than in the study of Bergknut. The Pfirmann grading system is based on the structure of the NP and the structure of the AF is not taken into account. It could be that with the use of another grading system that also focuses on the AF, a positive correlation is seen between GAG content and stage of degeneration.

In contrast to the NP, a higher DNA content in herniated samples of CD dogs compared to the other groups cannot be observed within the AF (figure 26 and 33). The large differences that are seen in the NP between the herniated CD samples and the other groups, do not exist in the AF. This contrast can be explained as follows: when the intervertebral disk degenerates, the AF weakens due to arising annular tears(P. N. Bergknut, 2011). This is a long-term process even though the intervertebral disks as a whole is classified by Pfirmann as an early stage of degeneration. This may be the reason for the fact that in the AF there are no large differences in DNA content between the different samples. Weakening of the AF may lead to herniation. In the NP we observed that herniated samples of CD dogs had higher DNA contents than the dogs of the other groups (figure 29). In CD dogs, herniation has a sudden unset(Hazewinkel et al., 2013) and if extrusion occurs, the NP is suddenly exposed to an inflammatory reaction. However, the AF of those samples is already changing for a longer period of time just like in the other groups. This might be the reason that in the AF we don't observe higher DNA contents in the herniated samples of CD dogs.

For further investigation, it would be interesting to add some 2NCD H AF samples to our dataset. This group is lacking, because during collecting our data we only selected on Pfirrmann grade and CD/NCD classification and in a later stage we divided samples in herniated and non-herniated. All of the collected 2NCD AF samples turned out to be non-herniated. 1NCD H samples are lacking as well, but those samples are rare because herniation in 1NCD dogs is very exceptional. Furthermore, some groups contain only one sample. It would be interesting to add more samples to our dataset. If the group sizes become larger, we can perform statistical analysis on the Pfirrmann grade to see whether there is significant evidence for a correlation between higher grades of disc degeneration and increased PGE2 levels.

COX-2 measurements

COX-2 positive cells should have an intense brownish color, as detected in the positive control. However, only very slight staining and a lot of background was observed in the patient samples. Antigen retrieval influences antigen-antibody binding and helps in optimizing the signal and minimizing the background. Therefore, I expect that antigen retrieval would improve the staining results. Because many different retrieval buffers and protocols exist, it is needed to sort out which buffer and protocol would be the best for our samples. Antigen-antibody binding can also be influenced by retrieval time, so it needs to be examined which antigen retrieval solution and time are best to optimize signal and minimize background. Hence, additional tests have to be performed to test series of experimental antigen retrieval procedures to further optimize the staining procedure. Unfortunately, these additive tests could not be part of my research project, due to time limitations, but are currently ongoing. Once the optimal procedure is found, the patient samples can be tested again to detect whether higher grades of disc degeneration are associated with higher COX-2 levels.

Conclusion

In conclusion, our dataset was too small to reliably test the correlation between PGE2 levels in IVDs of dogs suffering from chronic low back pain and higher grades of disc degeneration. A difference was found between PGE2/weight ratios and PGE2/DNA ratios, which can be explained by the cellularity of the samples. In this study the weight of the samples appeared to be a better correction factor for the PGE2 content. Inflammation could increase the cellularity of the sample, and DNA as a correction factor may therefore underestimate the PGE2 content. The PGE2/protein content ratio is not a reliable measure to represent PGE2 contents in this study. Inflammation increases the total protein content and therefore PGE2 levels may be underestimated. The PGE2 content in the nucleus pulposus appeared to be higher than in the annulus fibrosus. Furthermore, the PGE2 content in non-patient material is low, which suggests that the lack of clinical signs is associated with a lower PGE2 content. We found that the mean GAG concentrations in the nucleus pulposus are negatively correlated with increasing degeneration, which supports the findings reported by Bergknut et al. However, we did not find an increase in GAG/weight ratio in the AF as degeneration increases. The COX-2 staining on histological slides appeared to be not specific enough. The procedure needs further optimization to detect whether higher grades of degeneration are associated with higher COX-2 levels in patient samples.

Acknowledgements

First I would like to thank Nicole Willems, my supervisor. Thanks for the support and the positive feedback you gave me. A negative characteristic of me is that I might doubt too soon whether what I do is good or not. The positive feedback you gave me helped me a lot! I appreciated your quick replies on my emails and you were always willing to help me, even though you were very busy with writing your own articles. You involved me in everything; for example taking me with you to the department of radiology.

I want to thank Jeannette Wolfswinkel, for helping me in the lab. I did not have any experience with working in the lab, and so you had to explain me everything. Thanks for listening to my stupid questions and for your endless patience, although you were very busy.

I want to say thanks to Saskia Plomp, who introduced me to the immunohistochemistry. In my eyes a very complicated working field. Thanks for teaching me the basics. Because you let me make mistakes and let me think about things myself before explaining, I learned a lot. Although I felt really insecure to do a staining all by myself, you pushed me to do things on my own and this really helped me to learn a lot.

I want to thank Marianna Tryfonidou, for here wise words and input. I really admire your knowledge and the ease in which you find an answer for everything. My discussion would not have been a good one without your help.

I'm very happy to have chosen for a research internship at this department. I feel like I have done a lot of things. I worked in the lab, I learned to interpret MRI and CT images, I learned how to work in Excel, how to analyze data and how to present them. I think I really gained a good impression of what it is to do research. Furthermore, when I started this internship I was a bit afraid because of the English language. However, each lab meeting this feeling decreased. It was a very good exercise for me to communicate in English. I'm a bit scared though for the presentation I have to give soon, but with all those nice people at the department I guess it won't be problem. Thanks to you all!

Attachments

Attachment 1: Overzicht verwerking IVDs

Samples:

1 **½ IVD voor histologie**
   1. HE staining (UMCU)
   2. Alcian blue/Picosirius red staining (pathologie UMCU)

2 **½ IVD voor biochemische bepalingen**
   1. RNA
   2. GAG
   3. DNA
   4. PGE2
   5. Cytokine bepaling

2.1 RNA > RNAse free!
- NP in 300µl RLT buffer + β-ME (beta-mercapto-ethanol) (10 ul/ml)
- AF in 300µl RLT buffer + β-ME (beta-mercapto-ethanol) (10 ul/ml)

2.2/2.3/2.4 Samples in Complete Lysis M; #04719964001 (Roche)
Lysis M buffer dient aangemaakt te worden: 1 tablet protease inhibitor in 10 ml buffer
- NP in 400µl Lysis M buffer
- AF in 750µl Lysis M buffer

Supernatanten:
- Samples op ijs meenemen vanuit het UMCU
- ***Samples ontdooid(!) wegen in weegkamer JDV (goed droog!)***
- Als goed ontdooid is, dan in tissuelyser:
  - Aanzetten (knop achterkant apparaat)
  - Steriel kogeltje toevoegen aan epje
  - 30s op 20 Hz (1)
  - 1 minuut koelen op ijs
  - 30s op 20Hz (2)
  - Kogeltje verwijderen met magneet
  - 15 min. 14.000G (max) @4C
- Supernatant afnemen: 150 ul cytokine protocol → in -80 bewaren (indien niet voldoende supernatant, dan 80 ul aliquoteren)
  Indien onvoldoende supernatant, dan in ieder geval aliquoteren voor PGE2 en zorgen dat er voldoende beschikbaar is voor GAG bepaling.
- Bewaren aliquots:
  * PGE2: -80

* Cytokines: -80
* GAG: -80

Samples PGE2

- ELISA 100ul sample in mono nodig
  (N.B.! hvh sup kan beperkt zijn bij sommige samples! ~180 ul)
- Lezen op: 405 (415)nm, subtract 595nm, Dual

Samples GAG and DNA

- Voeg Papain digestie mix toe aan de pellet (SOP059) → voldoende papaine/cysteine aanwezig?

<u>Benodigd aan buffer:</u>

Pellet:

- Vul de pellet van de NP aan tot 500µl met papaine digestie buffer.
- Vul de pellet van de AF aan tot 1000µl met papaine digestie buffer.
- Supernatant 1:10 verdunnen in papaine digestie buffer (10 ul sample + 90 ul papaine digestiebuffer)
- Digesteer Pellet en Supernatant O/N bij 60˚C.

- **2.4 GAG**
  - Verdun gedigesteerde pellets 1:1001 in PBS-EDTA (10ul + 100ul PBS-EDTA en 10ul+ 900ul PBS-EDTA)
  - Supernatant digest 1:150 verdunnen in PBS-EDTA (10ul + 1490 ul PBS-EDTA)
  - Lezen op: 540nm and 595nm
- **2.5 DNA**
  - **Qubit** assay (JDV)
  - Supernatant niet bepalen.
  - 5 ul sample (gedigesteerd pellet) in 195 ul working solution (1:40)

2.6 Cytokine bepaling

- Filteren door spin-x filter (0.22 um nylon, costar #8169)) 150 ul supernatant en 2x 60 ul aliquoteren
- 2 min 14.000 G (max) @ 4C
- Indien filter verstopt: overbrengen in nieuw filter en nogmaals afdraaien

3 Store samples:

<u>- 80 Freezer UMCU</u>

* pellet in papain
* supernatant
* 2x 60 ul aliquot cytokine assay

Remark:

Geen volumes kleiner dan 10ul pipetteren. Dus als er een 1:1000 verdunning gemaakt moet worden, maak deze in twee keer.

Attachment 2: DMMB assay

FVM-UU, 25-11-2013

Background

The DMMB assay is the most commonly used method to quantify glycosaminoglycans (GAGs). The dimethylmethylene blue (DMMB) substance associates with repeating negative charges (sulphates) on the GAGs, after which a shift in the absorption maximum can be observed.

Chemicals

- 2* papain buffer (protein fridge)
  - 100 mL
    - 3.13 g H_2NaPO_4*2 H_2O (B16)
    - 0.326 g EDTA (B22)
    - Adjust to pH 6
- Papain digestion solution
  - Per mL of 2* papain buffer
    - 1.57 mg cysteine HCl (cold room)
    - 250 µg papain (Sigma, fluid 21 mg/mL) (cold room)
- PBS-EDTA in distilled water (cold room)
  - 250 mL
    - 1.42 g Na_2HPO_4 (B23)
    - 2.07 g H_2NaPO_4*2 H_2O (B16)
    - 0.93 g Na_2EDTA*2 H_2O (B228)
- DMMB Staining solution in distilled water (cold room)
  - 250 mL
    - 4 mg DMMB in 1.25 ml 100% ethanol, incubated for 2-16 hours (=stock). Store light protected, stable for 3 months.
    - 0.59 g NaCl (B20)
    - 0.76 g Glycine (B17)
- Chondroitin sulphate C 0.5mg/ml in PBS (C4384-250mg, Sigma) (cold room)
- The plates and other DMMB waste can be disposed in a chemical waste bin of cat. III after use.

Procedure

1. Digest your samples (if tissue/pellet) using the papain digestion solution. Incubate overnight at 60°C. Centrifuge the next day and incubate for an additional hour.

- 75 µL/micro-aggregate
- 200 µL/cell culture pellet
- 500 uL/NP
- 750 ul/AF
- Dilute NP/AF supernatant 1:10 with papain digestion solution

2. Dilute the chondroitin sulphate C (0,5mg/ml) standard 1:50 in PBS-EDTA.
3. Pipette 100µl in duplo of the diluted standard in the wells according to the following pipette scheme:

Well nr	ul CS 50x diluted	ul PBS-EDTA/Medium	= ug CS/well
1	0	100	0
2	3.125	96.875	0.03125
3	6.25	93,75	0.0625
4	12.5	87.5	0.125
5	25	75	0.25
6	50	50	0.50
7	75	25	0.75
8	100	0	1.00

4. Dilute the samples in PBS-EDTA.
    - Micro-aggregates: 1:25 (for control, TGFβ etc)
    - Micro-aggregates: 1:100 (for NCCM treated micro-aggregates)
    - Cell culture medium pellets: 1:50
    - Cell culture pellets: 1:50
    - Digested NP and AF pellet: 1:1000
    - Tissue supernatant: 1:150
5. Pipette 100µl of the diluted sample in the plate.
6. Add 200µl DMMB staining solution to each well.
7. Measure the extinction as soon as possible at 540 and 595nm (IRAS, 1.041). Contact person: Marjolein Oosterveer (tel 5958)

- Put on the computer and reader at least 20 minuted before measuring.
- ”Microplate reader”
- File : new read…. Endpoint
- Reading parameters: single or dual (dual: measurements directly corrected)
- Wavelength: 540 en 595 nm
- Mix plate 3 seconds
- Run
- Save via File… Export to C:DATA plate reader
- Short name (max 8 charakters) for the .txt file

8. Calculate the total GAG in each sample.
    - Divide the 540nm measurement through the 595nm measurement. Extract the blank. Make a plot of the sample and add a trend line with polynomic properties.
    - Calculate the amount of GAG according to the polynomic formula ($y=ax^2+bx+c$).
    - In excel this is expressed as = (-b+(root((b^2)-4*a*(c-y))))/(2*a).

Attachment 3: Immunohistochemic COX-2 staining protocol

- Dehydrate paraffin sections in:
  - Xylene 2 times 5 min
  - 100% EtOH 2 times 3 min
  - 96% EtOH 2 times 1 min
  - 70% EtOH 2 times 1 min
- Put the slides in demineralised water
- Make circles around tissue with Pap-pen
- Keep the tissue from drying out, add TBS or PBS on slides
- Touch the slides dry and put ready-made endogen peroxide on the slides (2 drops) 10min
- First touch the slides dry, then rinse the slides with TBS-T 2x5min
- Block in TBS-BSA 5% , 100µl
  60 min @ RT
- Don't rinse slides, but touch carefully dry
- Incubate slides with primary antibody COX-2 (Cayman clone CX229) by 4˚C
  1:800 in TBS-BSA 5%. - 100 µl O/N

Continuation next day:

- Rinse 2 times with TBS-T 5 min
- Incubate slides with Envision HRP (Dako K4007) 100µl 30 min @ RT
- Rinse 2 times with TBS 5 min
- Incubate slides with DAB 5 min @ RT
- Rinse 2 times with RX- water 5 min
- Counterstain with haematoxylin 10-30sec
- Rinse with running Tap-water 5-10 min
- Hydrate paraffin sections in:
  - 70% EtOH 2 times 1 min
  - 96% EtOH 2 times 1 min
  - 100% EtOH 2 times 3 min
  - Xylene 2 times 5 min
- Coverslip with permanent mounting medium

AB is stored in freezer

Preparing Solutions

DAB solution
- 4,5 ml PBS
- 500 µl DAB 10x stocksolution
- 5 µl H_2O_2 30%
- Filter

Tris HCL 1M
- 1 L demi water
- 30,3 gram Tris
- Add Ph. to 7,5 with HCL

TBS
- 1 L demi water
- 40ml of 1M Tris/HCL Ph. 7,5
- 8,766 gram NaCl

TBS-T 0,1%
- 1L TBS
- 1ml Tween20

TBS-BSA 5%
- 10 ml TBS
- 0,5gr BSA

Citrate buffer 0.01M
- 1 L MQ
- Add 2,941gr sodium citrate, stir for 15min
- Ph. 6.0, acidify with 1,0M citric acid

Attachment 4: Product information COX-2 monoclonal antibody

Product Information

COX-2 Monoclonal Antibody (Clone CX229)

Item No. 160112

Contents: This vial contains 50 µg lyophilized IgG_1. Resuspend the IgG_1 in 100 µl of purified water prior to use. Buffer will be 1X PBS.

Synonyms: Cyclooxygenase-2, Prostaglandin H Synthase 2

Antigen: Synthetic peptide from human COX-2 sequence amino acid 580-599 (NASSSRSGLDDINPTVLLKE). Homology of peptide antigen with COX-2 from other species:

Human	N A S S S R S G L D D I N P T V L L K
Bovine	N A S S S h S G L D D I N P T V L L K E
Canine	N A S S S r S G L D D I N P T V L L K E
Ovine	N A S S S h S G L D D I N P T V L L K

Host: Mouse, clone CX229

Cross Reactivity: (+) human, ovine, and monkey COX-2,[1] expected to react with bovine and canine COX-2, (-) mouse, rat, and rabbit COX-2 and COX-1 (all species)

Stability: ≥3 years at -20°C

Applications: Western blot (WB) and immunohistochemistry (IHC); the recommended starting dilution for WB is 0.5 µg/ml (1:1,000) and 1:50 to 1:100 for IHC. Other applications were not attempted and therefore optimal working dilutions should be determined empirically.

This vial contains lyophilized IgG against a KLH-conjugated peptide from human COX-2. For long term storage, we suggest the antibody be stored as supplied at -20°C. It will be stable for approximately three years. Reconstitute the contents of the vial with 100 µl of distilled water to make a 0.5 mg/ml stock solution. If the reconstituted antibody cannot be used within two weeks, it should be aliquoted into smaller vials (10 µl per vial works well) and stored at -20°C. For immunoblotting experiments, dilute 10 µl of the reconstituted antibody to 10 ml (1:1,000) with any buffer suitable for your experiment. For other applications the working concentration of the antibody must be determined empirically.

Cyclooxygenase (COX) catalyzes the first step in the biosynthesis of prostaglandins (PGs), thromboxanes, and prostacyclins: the conversion of arachidonic acid to PGH_2. Recent discoveries of the induction of COX biosynthesis by a variety of stimuli such as phorbol esters, lipopolysaccharides, and cytokines led to the hypothesis that the inducible form of cyclooxygenase, COX-2, is responsible for the biosynthesis of PGs under acute inflammatory conditions.[2] COX-2 is a 72 kDa protein which has been cloned from a variety of species including human, mouse, rat, and sheep.[3-6]

Lane 1: Recombinant human COX-2 (Cos-1 cell lysate)
Lane 2: Ovine COX-2 (microsomal fraction)

References

1. Duffy, D.M. and Stouffer, R.L. *Molecular Human Reproduction* **7(8)**, 731-739 (2001).
2. Xie, W., Chipman, J.G., Robertson, D.L., *et al. Proc. Natl. Acad. Sci USA* **88**, 2692-2696 (1991).
3. Hla, T. and Neilson, K. *Proc. Natl. Acad. Sci. USA* **89**, 7384-7388 (1992).
4. Kujubu, D.A., Fletcher, B.S., Varnum, B.C., *et al. J. Biol. Chem.* **266**, 12866-12872 (1991).
5. Yamagata, K., Andreasson, K.I., Kaufmann, W.E. *et al. Neuron* **11**, 371-386 (1993).
6. Zhang, Y., O'Sullivan, M., Hussain, H., *et al. Biochem. Biophys. Res. Commun.* **227**, 499-506 (1996).

Related Products

For a list of related products please visit: www.caymanchem.com/catalog/160112

Cayman Chemical

Mailing address
1180 E. Ellsworth Road
Ann Arbor, MI
48108 USA

Phone
(800) 364-9897
(734) 971-3335

Attachment 5: ENZO manual PGE2 high sensitivity EIA kit

Enzo® Life Sciences
Enabling Discovery in Life Sciences®

PGE_2 high sensitivity EIA kit

Catalog No. ADI-930-001

96 Well Kit

FOR RESEARCH USE ONLY. NOT FOR USE IN DIAGNOSTIC PROCEDURES.

ALEXIS assay designs BIOMOL Stressgen
www.enzolifesciences.com

Description

The PGE2 high sensitivity kit is a competitive immunoassay for the quantitative determination of Prostaglandin E_2 in biological fluids. Please read the complete kit insert before performing this assay. The kit uses a monoclonal antibody to PGE_2 to bind, in a competitive manner, the PGE_2 in the sample or an alkaline phosphatase molecule which has PGE_2 covalently attached to it. After a simultaneous incubation at 4ºC the excess reagents are washed away and substrate is added. After an incubation at 37ºC, the enzyme reaction is stopped and the yellow color generated is read on a microplate reader at 405nm. The intensity of the bound yellow color is inversely proportional to the concentration of PGE_2 in either standards or samples. The measured optical density is used to calculate the concentration of PGE_2. For further explanation of the principles and practice of immunoassays please see the excellent books by Chard[1] or Tijssen[2].

Introduction

Prostaglandin E_2 is formed in a variety of cells from PGH_2, which itself is synthesized from arachidonic acid by the enzyme prostaglandin synthetase[3-6]. PGE_2 has been shown to have a number of biological actions, including vasodilation[7], both anti- and proinflammatory action[8,9], modulation of sleep/wake cycles[10], and facilitation of the replication of human immunodeficiency virus[11]. It elevates cAMP levels[12] and stimulates bone resorption[13], and has thermoregulatory effects. It has been shown to be a regulator of sodium excretion and renal hemodynamics[14].

Prostaglandin E2

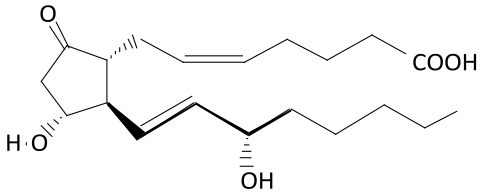

Precautions

FOR RESEARCH USE ONLY. NOT FOR USE IN DIAGNOSTIC PROCEDURES.

1. Some kit components contain azide, which may react with lead or copper plumbing. When disposing of reagents always flush with large volumes of water to prevent azide build-up.

2. Stop Solution is a solution of trisodium phosphate. This solution is caustic; care should be taken in use.
3. The activity of the alkaline phosphatase conjugate is dependent on the presence of Mg^{2+} and Zn^{2+} ions. The activity of the conjugate is affected by concentrations of chelators (>10 mM) such as EDTA and EGTA.
4. We test this kit's performance with a variety of samples, however it is possible that high levels of interfering substances may cause variation in assay results.
5. The Prostaglandin E_2 Standard provided, Catalog No. 80-0004, is supplied in ethanolic buffer at a pH optimized to maintain PGE_2 integrity. Care should be taken handling this material because of the known and unknown effects of prostaglandins.

Materials Supplied

1. **Goat anti-Mouse IgG Microtiter Plate, One Plate of 96 Wells, Catalog No. 80-0050** A plate using break-apart strips coated with goat antibody specific to mouse IgG.
2. **PGE_2 HS-EIA Conjugate, 6 mL, Catalog No. 80-0287** A blue solution alkaline phosphatase conjugated with PGE_2.
3. **PGE_2 HS-EIA Antibody, 6 mL, Catalog No. 80-0286** A yellow solution of a monoclonal antibody to PGE_2.
4. **Assay Buffer, 30 mL, Catalog No. 80-0010**
   Tris buffered saline containing proteins and sodium azide as preservative.
5. **Wash Buffer Concentrate, 30 mL, Catalog No. 80-1286**
   Tris buffered saline containing detergents.
6. **Prostaglandin E_2 Standard, 0.5 mL, Catalog No. 80-0004**
   A solution of 50,000 pg/mL PGE_2.
7. **pNpp Substrate, 20 mL, Catalog No. 80-0075**
   A solution of p-nitrophenyl phosphate in buffer. Ready to use.
8. **Stop Solution, 5 mL, Catalog No. 80-0247**
   A solution of trisodium phosphate in water. Keep tightly capped. Caution: **Caustic.**
9. **PGE_2 Assay Layout Sheet, 1 each, Catalog No. 30-0082**
10. **Plate Sealers, 2 each, Catalog No. 30-0012**

Storage

All components of this kit, **except the Conjugate and Standard**, are stable at 4°C until the kit's expiration date. The Conjugate and Standard **must** be stored at -20°C.

Materials Needed but Not Supplied

1. Deionized or distilled water.
2. Precision pipets for volumes between 5 µL and 1,000 µL.
3. Repeater pipets for dispensing 50 µL and 200 µL.
4. Disposable beakers for diluting buffer concentrates.
5. Graduated cylinders.
6. A 37 °C Incubator.
7. Adsorbent paper for blotting.
8. Microplate reader capable of reading at 405 nm, preferably with correction between 570 and 590 nm.

Sample Handling

The PGE_2 high sensitivity EIA is compatible with PGE_2 samples in a wide range of matrices after dilution in Assay Buffer. Please refer to the Sample Recovery recommendations on page 11 for details of suggested dilutions. However, the end user **must verify** that the recommended dilutions are appropriate for their samples. **Samples containing mouse IgG may interfere with the assay.**

Samples in the majority of tissue culture media, including those containing fetal bovine serum, can also be read in the assay, provided the standards have been diluted into the tissue culture media instead of Assay Buffer. There will be a small change in binding associated with running the standards and samples in media. Users should only use standard curves generated in media or buffer to calculate concentrations of PGE_2 in the appropriate matrix. For tissue, urine and plasma samples, prostaglandin synthetase inhibitors such as indomethacin or meclofenamic acid at concentrations up to 10 µg/mL should be added to either the tissue homogenate or urine and plasma samples.

Some samples normally have very low levels of PGE_2 present and extraction may be necessary for accurate measurement. A suitable extraction procedure is outlined below:

Materials Needed

1. PGE_2 Standard to allow extraction efficiency to be accurately determined. 2. 2M hydrochloric acid, deionized water, ethanol, hexane and ethyl acetate.
3. 200 mg C_{18} Reverse Phase Extraction Columns.

Procedure

1. Acidify the plasma, urine or tissue homogenate by addition of 2M HCl to pH of 3.5. Approximately 50 µL of HCl will be needed per mL of plasma. Allow to sit at 4 °C for 15 minutes. Centrifuge samples in a microcentrifuge for 2 minutes to remove any precipitate.
2. Prepare the C_{18} reverse phase column by washing with 10 mL of ethanol followed by 10 mL of deionized water.
3. Apply the sample under a slight positive pressure to obtain a flow rate of about 0.5 mL/minute. Wash the column with 10 mL of water, followed by 10 mL of 15% ethanol, and finally 10 mL hexane. Elute the sample from the column by addition of 10 mL ethyl acetate.
4. If analysis is to be carried out immediately, evaporate samples under a stream of nitrogen. Add at least 250 µL of Assay Buffer to the dried samples. Vortex well then let sit for five minutes at room temperature. Repeat twice more. If analysis is to be delayed, store samples as the eluted ethyl acetate solutions at -80 °C until the immunoassay is to be run.

Please refer to references 15-18 for details of extraction protocols.

Procedural Notes

1. Do not mix components from different kit lots or use reagents beyond the kit expiration date.
2. Allow all reagents to warm to room temperature for at least 30 minutes before opening.
3. Standards can be made up in either glass or plastic tubes.
4. Pre-rinse the pipet tip with the reagent, use fresh pipet tips for each sample, standard and reagent.
5. Pipet standards and samples to the bottom of the wells.
6. Add the reagents to the side of the well to avoid contamination.
7. This kit uses break-apart microtiter strips, which allow the user to measure as many samples as desired. Unused wells must be kept desiccated at 4 °C in the sealed bag provided. The wells should be used in the frame provided.
8. **Care must be taken to minimize contamination by endogenous alkaline phosphatase.** Contaminating alkaline phosphatase activity, especially in the substrate solution, may lead to high blanks. Care should be taken not to touch pipet tips and other items that are used in the assay with bare hands.

9. **Prior to addition of substrate, ensure that there is no residual wash buffer in the wells. Any remaining wash buffer may cause variation in assay results.**

Reagent Preparation

1. PGE_2 Standard

Allow the 50,000 pg/mL PGE_2 standard solution to warm to room temperature. Label eight 12 x 75 mm glass tubes #1 through #8. Pipet 1 mL of standard diluent (Assay Buffer or Tissue Culture Media) into tube #1. Pipet 500 µL of diluent into tubes #2 through #8. Remove 20 µL of diluent from tube #1.

Add 20 µL of the 50,000 pg/mL standard to tube #1. Vortex thoroughly. Add 500 µL of tube #1 to tube #2 and vortex thoroughly. Add 500 µL of tube #2 to tube #3 and vortex. Continue this for tubes #4 through #8.

The concentration of PGE_2 in tubes #1 through #8 will be 1,000, 500, 250, 125, 62.5, 31.25, 15.63, and 7.81 pg/mL, respectively. See PGE_2 Assay Layout Sheet for dilution details.

Diluted standards should be used within 60 minutes of preparation.

2. PGE_2 Conjugate

Allow the conjugate to warm to room temperature. Any unused conjugate should be aliquoted and re-frozen at or below -20 °C.

3. Wash Buffer

Prepare the Wash Buffer by diluting 5 mL of the supplied concentrate with 95 mL of deionized water. This can be stored at room temperature until the kit expiration date, or for 3 months, whichever is earlier.

Assay Procedure

Bring all reagents to room temperature for at least 30 minutes prior to opening.

All standards and samples should be run in duplicate.

1. Refer to the Assay Layout Sheet to determine the number of wells to be used and put any remaining wells with the desiccant back into the pouch and seal the ziploc. Store unused wells at 4°C.
2. Pipet 100 µL of standard diluent (Assay Buffer or Tissue Culture Media) into the NSB and the Bo (0 pg/mL Standard) wells.
3. Pipet 100 µL of Standards #1 through #8 into the appropriate wells.
4. Pipet 100 µL of the Samples into the appropriate wells.
5. Pipet 50 µL of Assay Buffer into the NSB wells.
6. Pipet 50 µL of blue Conjugate into each well, except the Total Activity (TA) and Blank wells.
7. Pipet 50 µL of yellow Antibody into each well, except the Blank, TA and NSB wells.

NOTE: Every well used should be **Green** in color except the NSB wells which should be **Blue**. The Blank and TA wells are empty at this point and have no color.

8. Incubate the plate overnight (18-24 hours) at 4°C. The plate should be covered with the plate sealer provided.
9. Empty the contents of the wells and wash by adding 400 µL of wash solution to every well. Repeat the wash 2 more times for a total of **3 Washes.**
10. After the final wash, empty or aspirate the wells, and firmly tap the plate on a lint free paper towel to remove any remaining wash buffer.
11. Add 5 µL of the blue Conjugate to the TA wells.

12. Add 200 µL of the pNpp Substrate solution to every well. Incubate at 37°C for 1 hour without shaking. The plate should be covered with the provided plate sealer.

13. Add 50 µL of Stop Solution to every well. This stops the reaction and the plate should be read immediately.

14. Blank the plate reader against the Blank wells, read the optical density at 405 nm, preferably with correction between 570 and 590 nm. If the plate reader is not able to be blanked against the Blank wells, manually subtract the mean optical density of the Blank wells from all readings.

Calculation of Results

Several options are available for the calculation of the concentration of PGE_2 in the samples. We recommend that the data be handled by an immunoassay software package utilizing a 4 parameter logistic curve fitting program. If data reduction software is not readily available, the concentration of PGE_2 can be calculated as follows:

1. Calculate the average net Optical Density (OD) bound for each standard and sample by subtracting the average NSB OD from the average OD bound:

   Average Net OD = Average Bound OD - Average NSB OD

2. Calculate the binding of each pair of standard wells as a percentage of the maximum binding wells (Bo), using the following formula:

   $$\text{Percent Bound} = \frac{\text{Net OD}}{\text{Net Bo OD}} \times 100$$

3. Using Logit-Log paper plot Percent Bound versus Concentration of PGE_2 for the standards. Approximate a straight line through the points. The concentration of PGE_2 in the unknowns can be determined by interpolation.

Typical Results

The results shown below are for illustration only and should not be used to calculate results.

Sample	Mean OD(-Blank)	Average Net OD	Percent Bound	**PGE_2 (pg/mL)**
Blank OD	(0.105)			
TA	2.406	2.301		
NSB	0.104	0.000	0.00%	
Bo	1.125	1.020	100%	**0**
S1	0.166	0.061	6.0%	**1,000**
S2	0.214	0.109	10.7%	**500**
S3	0.269	0.164	16.1%	**250**
S4	0.378	0.273	26.8%	**125**
S5	0.567	0.462	45.3%	**62.5**
S6	0.684	0.579	56.8%	**31.25**
S7	0.811	0.706	69.2%	**15.63**
S8	0.994	0.889	87.2%	**7.81**
Unknown 1	0.283	0.178	17.5%	**260**
Unknown 2	0.489	0.384	37.7%	**76**

Typical Standard Curve

A typical standard curve is shown below. This curve **must not** be used to calculate PGE_2 concentrations; each user must run a standard curve for each assay.

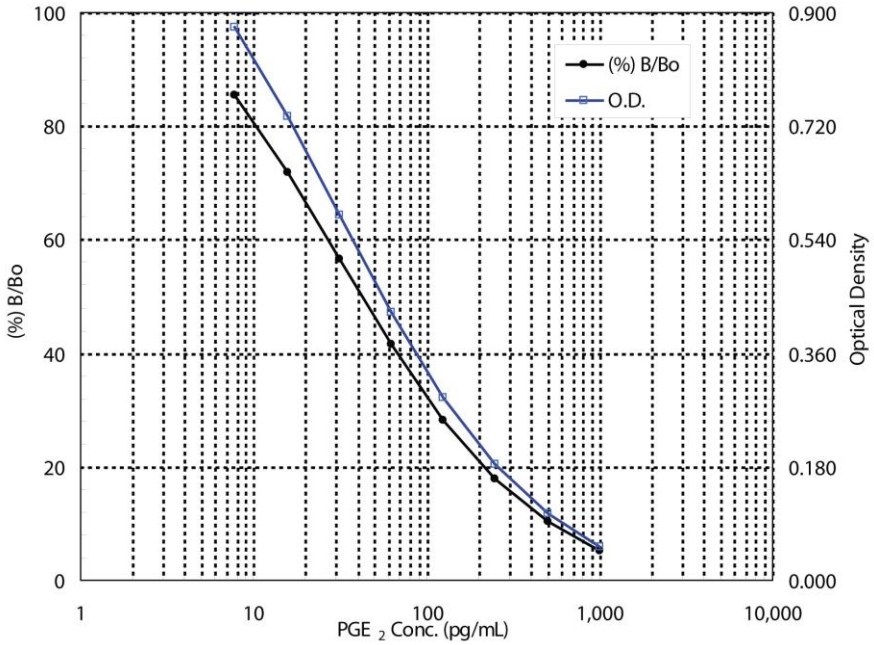

Typical Quality Control Parameters

Total Activity Added	=	2.406 x 10 = 24.06
%NSB	=	0.0%
%Bo/TA	=	4.2%
Quality of Fit	=	1.0 (Calculated from 4 parameter logistic curve fit)
20% Intercept	=	215 pg/mL
50% Intercept	=	42 pg/mL
80% Intercept	=	11 pg/mL

Performance Characteristics

The following parameters for this kit were determined using the guidelines listed in the National Committee for Clinical Laboratory Standards (NCCLS) Evaluation Protocols[19].

Sensitivity

Sensitivity was calculated by determining the average optical density bound for sixteen (16) wells run as Bo, and comparing to the average optical density for sixteen (16) wells run with Standard #8. The detection limit was determined as the concentration of PGE_2 measured at two (2) standard deviations from the zero along the standard curve. The value was determined to be 8.26 pg/mL.

Linearity

A sample containing 200 pg/mL PGE_2 was diluted 4 times 1:2 in the kit Assay Buffer and measured in the assay. The data was plotted graphically as actual PGE_2 concentration versus measured PGE_2 concentration.

The line obtained had a slope of 1.069 and a correlation coefficient of 1.000.

Precision

Intra-assay precision was determined by taking samples containing low, medium and high concentrations of PGE_2 and running these samples multiple times (n=24) in the same assay. Inter-assay precision was determined by measuring three samples with low, medium and high concentrations of PGE_2 in multiple assays (n=8).

The precision numbers listed below represent the percent coefficient of variation for the concentrations of PGE_2 determined in these assays as calculated by a 4 parameter logistic curve fitting program.

	PGE_2	Intra-assay	Inter- assay
	(pg/mL)	%CV	%CV
Low	19	9.8	
Medium	56	6.1	
High	110	3.1	
Low	17		12.1
Medium	51		12.6
High	98		8.1

Cross Reactivities

The cross reactivities for a number of related eicosanoid compounds was determined by dissolving the cross reactant (purity checked by N.M.R. and other analytical methods) in Assay Buffer at concentrations from 500,000 to 39 pg/mL. These samples were then measured in the PGE_2 assay, and the measured PGE_2 concentration at 50% B/Bo calculated. The % cross reactivity was calculated by comparison with the actual concentration of cross reactant in the sample and expressed as a percentage.

Compound	Cross Reactivity
PGE_2	100%
PGE_1	70%
PGE_3	16.3%
$PGF_{1\alpha}$	1.4%
$PGF_{2\alpha}$	0.7%
6-keto-$PGF_{1\alpha}$	0.6%
PGA_2	0.1%
PGB_1	0.1%
13,14-dihydro-15-keto-$PGF_{2\alpha}$	<0.1%
6,15-keto-13,14-dihydro-$PGF_{1\alpha}$	<0.1%
Thromboxane B_2	<0.1%
2-Arachidonoylglycerol	<0.1%
Anandamide	<0.1%
PGD_2	<0.1%
Arachadonic Acid	<0.1%

Sample Recoveries

Please refer to pages 4 and 5 for Sample Handling recommendations and Standard Preparation.

PGE_2 concentrations were measured in a variety of different samples including tissue culture media, human saliva, serum, and urine. PGE_2 was spiked into the undiluted samples of these media which were then diluted with the appropriate diluent and assayed in the kit. The following results were obtained:

Sample	**% Recovery***	**Recommended Dilution***

Tissue Culture Media	104.4	None
Human Saliva	123.3	1:10
Human Urine	108.9	1:10
Human Male Serum	126.1	1:10
Human Female Serum	113.7	1:10
Human Whole Blood	101.2	1:10

* See Sample Handling instructions on page 4 for details.

References

1. T. Chard, "An Introduction to Radioimmunoassay & Related Techniques 4th Ed.,", (1990) Amsterdam: Elsevier.
2. P. Tijssen,"Practice & Theory of Enzyme Immunoassays", (1985) Amsterdam: Elsevier.
3. P.W. Ramwell, Biol. Reprod., (1977) 16: 70.
4. R.J. Flower & G.J. Blackwell, Biochem. Pharm., (1976) 25: 285.
5. S. Moncada & J.R. Vane, Pharm. Rev., (1979) 30: 293.
6. B. Sameulsson, et al., Ann. Rev Biochem., (1978) 47: 997.
7. P.D.I. Richardson, et al., Brit. J. Pharmacol., (1976) 57: 581.
8. J. Raud, et al., Proc. Natl. Acad. Sci., USA, (1988) 85: 2315.
9. J.W. Christman, et al., Prostaglandins, (1991) 41: 251.
10. O. Hayaishi, J. Biol. Chem., (1988) 263: 14593.
11. S. Kuno, et al., Proc. Natl. Acad. Sci., USA, (1986) 83: 3487.
12. D.L. Bareis, et al., Proc. Natl. Acad. Sci., USA, (1983) 80: 2514.
13. L.G. Raisz, et al., Nature, (1977) 267: 532.
14. C.R. Long, et al., Prostaglandins, (1990) 40: 591.
15. K. Green, et al., Anal. Biochem, (1973) 54: 434.
16. J. Frolich, et al., J. Clin. Invest., (1975) 55: 763.
17. J.E. Shaw & P.W. Ramwell, Meth. Biochem. Anal., (1969) 17: 325.
18. K. Green, et al., Adv. Prostaglandin & Thromboxane Res., (1978) 5: 15.
19. National Committee for Clinical Laboratory Standards Evaluation Protocols, SC1, (1989) Villanova, PA: NCCLS.

Enzo® Life Sciences
Enabling Discovery in Life Sciences®

Use of Product

This product contains research chemicals. As such, they should be used and handled only by or under the supervision of technically qualified individuals. This product is not intended for diagnostic or human use.

www.enzolifesciences.com

Enabling Discovery in Life Science®

Warranty

Enzo Life Sciences International, Inc. makes no warranty of any kind, expressed or implied, which extends beyond the description of the product in this brochure, except that the material will meet our specifications at the time of delivery. Enzo Life Sciences International, Inc. makes no guarantee of results and assumes no liability for injuries, damages or penalties resulting from product use, since the conditions of handling and use are beyond our control.

North/South America
ENZO LIFE SCIENCES INT'L, INC.

Germany
ENZO LIFE SCIENCES GmbH

UK & Ireland
ENZO LIFE SCIENCES (UK) LTD.

5120 Butler Pike
Plymouth Meeting, PA 19462-1202/USA
Tel. 1-800-942-0430/(610)941-0430
Fax (610) 941-9252
info-usa@enzolifesciences.com

Marie-Curie-Strasse 8
DE-79539 Lorrach / Germany
Tel. +49/0 7621 5500 526
Toll Free 0800 664 9518
Fax +49/0 7621 5500 527
info-de@enzolifesciences.com

Palatine House
Matford Court
Exeter EX2 8NL / UK
Tel. 0845 601 1488 (UK customers)
Tel. +44/0 1392 825900 (overseas)
Fax +44/0 1392 825910
info-uk@enzolifesciences.com

Switzerland & Rest of Europe
ENZO LIFE SCIENCES AG
Industriestrasse 17, Postfach
CH-4415 Lausen / Switzerland
Tel. +41/0 61 926 89 89
Fax +41/0 61 926 89 79
Info-ch@enzolifesciences.com

Benelux
ENZO LIFE SCIENCES BVBA
Melkerijweg 3
BE-2240 Zandhoven / Belgium
Tel. +32/0 3 466 04 20
Fax +32/0 3 466 04 29
info-be@enzolifesciences.com

France
ENZO LIFE SCIENCES
c/o Covalab s.a.s.
13, Avenue Albert Einstein
FR-69100 Villeurbanne / France
Tel. +33 472 440 655
Fax +33 437 484 239
Info-fr@enzolifesciences.com

Attachment 6: Manual Qubit® dsDNA BR Assay Kits

For use with the Qubit® 2.0 Fluorometer, Catalog nos. Q32850, Q32853

invitrogen™

Qubit® dsDNA BR Assay Kits

For use with the Qubit® 2.0

Fluorometer **Catalog nos.** Q32850,

Q32853

Table 1. Contents and storage information

Material	Amount	Concentration	Storage	Stability
Qubit® dsDNA BR reagent (Component A)	250 µL or 1.25 mL	200X concentrate in DMSO	Room temperature Desiccate Protect from light	When stored as directed, kits are stable for 6 months
Qubit® dsDNA BR buffer (Component B)	50 mL or 250 mL	NA	• Room temperature	
Qubit® dsDNA BR standard #1 (Component C)	1 mL or 5 mL	0 ng/µL in TE buffer	• ≤4°C	
Qubit® dsDNA BR standard #2 (Component D)	1 mL or 5 mL	100 ng/µL in TE buffer		

NA = Not applicable.

Introduction

The Qubit® dsDNA BR Assay Kits for use with the Qubit® 2.0 Fluorometer make DNA quantitation easy and accurate. The kit provides concentrated assay reagent, dilution buffer, and pre-diluted DNA standards. Simply dilute the reagent using the buffer provided, add your sample (any volume from 1–20 µL is acceptable), then read the concentration using the Qubit® 2.0 Fluorometer. The assay is highly selective for double-stranded DNA (dsDNA) over RNA (*Appendix*, Figure 1) and is accurate for initial sample concentrations from 100 pg/µL to 1000 ng/µL. The assay is performed at room temperature, and the signal is stable for 3 hours. Common contaminants, such as salts, free nucleotides, solvents, detergents, or protein are well tolerated in the assay (*Appendix*, Table 2). In addition to the Qubit® dsDNA BR Assay Kits described here, we offer other kits for assaying RNA, protein, and dsDNA at a lower concentration range (*Appendix*, Table 3).

To determine the purity of your sample, use the Qubit® dsDNA BR Assay Kit together with the Qubit® RNA Assay Kit. These measurements will give you a much better indication of sample purity than that produced by an A_{260}/A_{280} measurement. To measure protein contamination in nucleic acid samples, simply run 1–20 µL of the sample in the Qubit® protein assay.

Materials required	
But not provided	Plastic container (disposable) for mixing the Qubit® working solution Qubit® assay tubes (500 tubes, Cat. no. Q32856) or Axygen® PCR-05-C tubes (VWR, part no. 10011-830)
dsDNA BR Assay Kits	The Qubit® dsDNA BR reagent and buffer are designed for room temperature storage. The Qubit® dsDNA BR reagent is supplied in DMSO, which freezes at temperatures lower than room temperature. Store the DNA standards at 4°C.

Assay temperature

The Qubit® dsDNA BR assay for the Qubit® 2.0 Fluorometer delivers optimal performance when all solutions are at room temperature (22–28˚C). The Qubit® assays were designed to be performed at room temperature, as temperature fluctuations can influence the accuracy of the assay (*Appendix*, Figure 2). To minimize temperature fluctuations, store the Qubit® dsDNA BR reagent and the Qubit® dsDNA BR buffer at room temperature and insert all assay tubes into the Qubit® 2.0 Fluorometer only for as much time as it takes for the instrument to measure the fluorescence; the Qubit® 2.0 Fluorometer can raise the temperature of the assay solution significantly, even over a period of a few minutes. Do not hold the assay tubes in your hand before reading, as this will warm the solution and result in a low reading.

The protocol below assumes that you will be preparing standards for calibrating the Qubit® 2.0 Fluorometer. If you plan to use the last calibration performed on the instrument, you will need fewer tubes (step 1.1) and less working solution (step 1.3). More detailed instructions on the use of the Qubit® 2.0 Fluorometer (corresponding to steps 1.9–1.12 and 2.1–2.6) can be found in the user manual accompanying the instrument. For sample purity determinations, it is possible to use the Qubit® 2.0 Fluorometer to calculate the amount of dsDNA and RNA in the same sample. Simply perform each assay for your sample.

To allow the Qubit® assay to reach maximum fluorescence, incubate the tubes for the DNA and RNA assays for 2 minutes after mixing the sample or standard with the working solution. After this incubation period, the fluorescence signal is stable for 3 hours at room temperature.

Photobleaching of the Qubit® reagent

The Qubit® reagents exhibit high photostability in the Qubit® 2.0 Fluorometer, showing <0.3% drop in fluorescence after 9 readings and <2.5% drop in fluorescence after 40 readings. It is important to remember, however, that if the assay tube remains in the Qubit® 2.0 Fluorometer for multiple readings, a temporary reduction in fluorescence will be observed as the solution increases in temperature (Appendix, Figure 2). Note that the temperature inside the Qubit® 2.0 Fluorometer may be as much as 3°C above room temperature after 1 hour. For this reason, if you want to perform multiple readings of a single tube, you should remove the tube from the instrument and let it equilibrate to room temperature for 30 seconds before taking another reading.

Calibrating the Qubit® 2.0 Fluorometer

For each assay, you have the choice to run a new calibration or to use the values from the previous calibration. As you first use the instrument, you should perform a new calibration each time. As you become familiar with the assays, the instrument, your pipetting accuracy, and significant temperature fluctuation within your laboratory, you should determine the level of comfort you have using the calibration data stored from the last time the instrument was calibrated. Remember also that the fluorescence signal in the tubes containing standards and the samples is stable for no longer than 3 hours. See Figure 3 in the Appendix for an example of the calibration curve used to generate the quantitation results.

1.1 Set up the required number of 0.5-mL tubes for standards and samples. The Qubit® dsDNA BR assay requires 2 standards.

Note: Use only thin-wall, clear, 0.5-mL PCR tubes. Acceptable tubes include Qubit® assay tubes (500 tubes, Cat. no. Q32856) or Axygen® PCR-05-C tubes (VWR, part no. 10011-830).

1.2 Label the tube lids.

Note: It is important to label the lid of each standard tube correctly as calibration of the Qubit® 2.0 Fluorometer requires that the standards be introduced to the instrument in the right order.

1.3 Make the Qubit® working solution by diluting the Qubit® dsDNA BR reagent 1:200 in Qubit® dsDNA BR buffer. Use a clean plastic tube each time you make the Qubit® working solution.

Do not mix the working solution in a glass container.

Note: The final volume in each assay tube must be 200 µL. Each standard tube requires 190 µL of Qubit® working solution, and each sample tube requires anywhere from 180–199 µL. Prepare sufficient Qubit® working solution to accommodate all standards and samples.

For example, for 8 samples, prepare enough working solution for the samples and 2 standards: ~200 µL per tube in 10 tubes yields 2 mL of working solution (10 µL of Qubit® reagent plus 1990 µL of Qubit® buffer).

1.4 Load 190 µL of Qubit® working solution into each of the tubes used for standards.

1.5 Add 10 µL of each Qubit® standard to the appropriate tube, then mix by vortexing 2–3 seconds. Be careful not to create bubbles.

Note: Careful pipetting is critical to ensure that exactly 10 µL of each Qubit® dsDNA BR standard is added to 190 µL of Qubit® working solution.

1.6 Load the Qubit® working solution into individual assay tubes so that the final volume in each tube after adding sample is 200 µL.

Note: Your sample can be anywhere from 1–20 µL, therefore, load each assay tube with a volume of Qubit® working solution anywhere from 180–199 µL.

1.7 Add each of your samples to assay tubes containing the correct volume of Qubit® working solution (prepared in step 1.6), then mix by vortexing 2–3 seconds. The final volume in each tube should be 200 µL.

1.8 Allow all tubes to incubate at room temperature for 2 minutes.

1.9 On the Home Screen of the Qubit® 2.0 Fluorometer, press **DNA**, then select **dsDNA Broad Range** as the assay type. The Standards Screen is displayed.

Note: If you have already performed a calibration for the selected assay, the Qubit® 2.0 Fluorometer prompts you to choose between reading new standards and using the previous calibration. See *Calibrating the Qubit® 2.0 Fluorometer* above for calibration guidelines.

1.10 On the Standards Screen, select to run a new calibration or to use the last calibration:

Press **Yes** to run a new calibration, then:

Insert the tube containing Standard #1 in the Qubit® 2.0 Fluorometer, close the lid, then press **Read**. The reading takes approximately 3 seconds. Remove Standard #1.Insert the tube containing Standard #2 in the Qubit® 2.0 Fluorometer, close the lid, then press **Read**. Remove Standard #2.

OR

Press **No** to use the last calibration. The Sample Screen is displayed. Insert a sample tube into the Qubit® 2.0 Fluorometer, close the lid, then press **Read**.

After the measurement is completed, the result is displayed on the screen.

Note: The value given by the Qubit® 2.0 Fluorometer at this stage corresponds to the concentration after your sample was diluted into the assay tube. You can record this value and perform the calculation yourself to find out the concentration of your original sample (see *Calculating the concentration of your sample* below) or the Qubit® 2.0 Fluorometer performs this calculation for you (see *Dilution Calculator* on page 5).

1.11 To read the next sample, remove the sample from the Qubit® 2.0 Fluorometer, insert the next sample, then press **Read Next Sample**.

1.12 Repeat sample readings until all samples have been read.

Calculating the concentration of your sample

The Qubit® 2.0 Fluorometer gives values for the Qubit® dsDNA BR assay in µg/mL. This value corresponds to the concentration after your sample was diluted into the assay tube. To calculate the concentration of your sample, use the following equation:

Concentration of your sample = QF value × $\left(\frac{200}{x}\right)$

where:

QF value = the value given by the Qubit® 2.0 Fluorometer

x = the number of microliters of sample you added to the assay tube

This equation generates a result with the same units as the value given by the Qubit® 2.0 Fluorometer (that is, if the Qubit® 2.0 Fluorometer gave a concentration in µg/mL, the result of the equation will be in µg/mL).

Dilution Calculator

The "Dilution Calculator" feature of the Qubit® 2.0 Fluorometer calculates the concentration of your original sample based on the volume of sample you added to the assay tube. To have the Qubit® 2.0 Fluorometer perform this calculation for you, follow the instructions below.

2.1 After the sample measurement is completed, press **Calculate Stock Conc.** The Dilution Calculator Screen containing the volume roller wheel is displayed.

2.2 Using the volume roller wheel, select the volume of your original sample that you added to the assay tube. When you stop scrolling, the Qubit® 2.0 Fluorometer calculates the original sample concentration based on the measured assay concentration.

2.3 To change the units in which the original sample concentration is displayed, press **µg/mL** A pop-up window opens, showing the current unit selection (indicated by a red dash).

2.4 Select the unit for your original sample concentration by touching the desired unit in the unit selection pop-up window. To close the unit selection pop-up window, touch anywhere on the screen outside the pop-up.

The Qubit® 2.0 Fluorometer automatically converts the units to your selection once the unit selection pop-up window is closed.

Note: The unit button next to your sample concentration reflects the change in the units (for example, if you change the unit to pg/µL, the button displays pg/µL).

2.5 To save the data from your calculation to the Qubit® 2.0 Fluorometer, press **Save** on the Dilution Calculator screen. The last calculated value of your measurement is saved in the *.csv file and tagged with a time and date stamp.

2.6 To exit the Dilution Calculator screen, press any navigator button on the bottom of the screen or **ReadNext Sample**.

Note: When you navigate away from the Dilution Calculator screen, the Qubit® 2.0 Fluorometer saves the last values for the sample volume and the units in the Dilution Calculator screen only. Returning to the Dilution Calculator screen displays these last selected values.

Attachment 7: Protocol for the measurement of proteins

from whole liver tissues using the DC Protein Assay from BioRad Laboratories

(Cat.# 500-0116)

Materials and methods:

- *DC* Protein Assay from BioRad Laboratories (Cat.# 500-0116).
- 1 x PBS
- Bovine Serum Albumin (BSA, Sigma A-9647) solution, 1.5 mg/ml in PBS

Protocol using a 96-well microplate:

Note: Warm all components at 37ºC for 5 minutes prior to use.

1. Preparation of working reagent, Add 20 ul of reagent S to each ml of reagent A (now called A*).
   - For 1.5 ml A* (needed for half a plate) add 30 ul reagent S to 1.5 ml of A.

2. Prepare 5 dilutions of BSA protein standard from 0.2 mg/ml to 1.5 mg/ml as following:

   Stock BSA 15 mg dissolved in 1 ml PBS, keep at 40ºC for few minutes.

   1. 50 ul stock BSA plus 450 ul PBS 1.50 mg/ml
   2. 83 ul 1 plus 17 ul PBS 1.25 mg/ml
   3. 67 ul 1 plus 33 ul PBS 1.00 mg/ml
   4. 50 ul 1 plus 50 ul PBS 0.75 mg/ml
   5. 33 ul 1 plus 67 ul PBS 0.50 mg/ml
   6. 17 ul 1 plus 83 ul PBS 0.25 mg/ml
   7. 0 ul 1 plus 100 ul PBS 0.00 mg/ml

3. Pipet 5 ul of Standard and Samples in a clean and dry microtiterplate in triplicate.

Note: Hepatocyte samples sometimes have to be diluted prior to use

4. Add 25 ul of Reagent A* into each well.
5. Add 200 ul of Reagent B into each well. If the micro plate reader has a mixing function available, place plate in reader and mix for 5 seconds. If not, gently agitate the plate to mix the reagents. If bubbles form pop them with a clean, dry pipet tip.
6. After 15 minutes, absorbance can be read at 750 nm (otherwise 650 - 750 nm). The absorbance will be stable for 1 hour.

Note: 1 mg aprotinin = 14 TIU (trypsin inh. units) = 5.900 KIU (kallikrein inh. units)

Attachment 8: DC Protein Assay Instruction Manual

DC Protein Assay Instruction Manual

For Technical Service Call Your Local Bio-Rad Office or in the U.S. Call **1-800-4BIORAD** (1-800-424-6723)

Section 1 Introduction and Principle

The Bio-Rad *DC* Protein Assay is a colorimetric assay for protein concentration following detergent solubilization. The reaction is similar to the well-documented Lowry[1] assay, but with the following improvements: The reaction reaches 90% of its maximum color development within 15 minutes thereby saving valuable time, and the color changes not more than 5% in 1 hour or 10% in 2 hours after the addition of reagents.

The assay is based on the reaction of protein with an alkaline copper tartrate solution and Folin reagent. As with the Lowry assay, there are two steps which lead to color development: The reaction between protein and copper in an alkaline medium, and the subsequent reduction of Folin reagent by the copper-treated protein.[1] Color development is primarily due to the amino acids tyrosine and tryptophan, and to a lesser extent, cystine, cysteine, and histidine.[1,2] Proteins effect a reduction of the Folin reagent by loss of 1, 2, or 3 oxygen atoms, thereby producing one or more of several possible reduced species which have a characteristic blue color with maximum absorbance at 750 nm and minimum absorbance at 405 nm.[2]

Section 2 Product Description

Reagent package (catalog number 500-0116) includes:

250 ml REAGENT A, an alkaline copper tartrate solution
2000 ml REAGENT B, a dilute Folin Reagent
5 ml REAGENT S
(Sufficient for 500 standard assays or 10,000 microplate assays)

The reagent package may be purchased as a kit with a bovine gamma globulin standard (kit catalog number 500-0111) or bovine serum albumin standard (kit catalog number 500-0112).

Section 3 Materials Required but Not Supplied

For standard assay:

13 x 100 mm test tubes

Reservoir for working reagent (size depends on amount of reagent that will be prepared)

Pipets accurately delivering 100 µl, 500 µl, and 4.0 ml

Graduated cylinders or pipets for reagent preparation

Spectrophotometer set to 750 nm

Vortex mixer

Plastic or glass cuvettes with 1 cm path length matched to laboratory spectrophotometer

Test tube rack to hold 13 x 100 mm test tubes

For microplate assay:

Microtiter plates

Reservoir for working reagent

Pipets for reagent preparation

Pipets accurately delivering 5 µl, 25 µl, and 200 µl

Microplate reader set to 750 nm

3.1 Safety Considerations

Eye protection and gloves should be worn while using this product. Consult MSDS at the end of this manual for additional information.

Section 4 Reagent Compatibility

The listed compounds were tested and found to be compatible with the BioRad *DC* Protein Assay. In some cases, the presence of one or more of these substances will effect a change in the response of the protein to the assay reagents; therefore, the standard should **always** be prepared in the same buffer as the sample.

10% SDS	1% CHAPS	2% NP-40
1% Triton† X-100	1% CHAPSO	1% Thesit†
1% Tween† 20	1% Octyl glucoside	1% Brij†-35
0.2% $C_{12}E_8$*	0.1 M Tris, pH 8	0.5 M NaOH
0.5 M HCl	0.5 M $(NH_4)_2SO_4$	0.025M EDTA
0.05 M $CaCl_2$	0.4 M Guanidine HCl	4 M Urea
0.05% Sodium azide	1 mM DTT (dithiothreitol)	

Note: The DC Protein Assay is incompatible with 2-mercaptoethanol (BME)

† BRIJ and TWEEN are registered trademarks of Atlas Chemical. THESIT is a registered trademark of Desitin Arzneimittel GMBH. TRITON is a registered trademark of Rohm and Haas.

*octaethyleneglycol dodecyl ether

Section 5 Instructions

5.1 Standard Assay Protocol

1. Preparation of working reagent

   Add 20 µl of reagent S to each ml of reagent A that will be needed for the run. (This **working reagent A'** is stable for one week even though a precipitate will form after one day. If precipitate forms, warm the solution and vortex. Do not pipet the undissolved precipitate, as this will likely plug the tip of the pipet, thereby altering the volume of reagent that is added to the sample.)

   If samples do not contain detergent, you may omit step #1 and simply use reagent A as supplied.

2. Prepare 3 - 5 dilutions of a protein standard containing from 0.2 mg/ml toabout 1.5 mg/ml protein. A standard curve should be prepared each time the assay is performed. *For best results, the standards should always be prepared in the same buffer as the sample.*
3. Pipet 100 µl of standards and samples into clean, dry test tubes.
4. Add 500 µl of reagent A' or A (see note from step 1) into each test tube.Vortex.
5. Add 4.0 ml reagent B into each test tube and vortex immediately.
6. After 15 minutes, absorbances can be read at 750 nm. The absorbances willbe stable at least 1 hour. (See Troubleshooting Guide for recommendation on using a wavelength other than 750 nm.)

5.2 Microplate Assay Protocol

1. Preparation of working reagent

   Add 20 µl of reagent S to each ml of reagent A that will be needed for the run. (This **working reagent A'** is stable for 1 week even though a precipitate will form after 1 day. If precipitate forms, warm the solution and vortex. Do not pipet the undissolved precipitate, as this will likely plug the tip of the pipet, thereby altering the volume of reagent that is added to the sample.)

   If samples do not contain detergent, you may omit step #1 and simply use reagent A as supplied.

2. Prepare 3 - 5 dilutions of a protein standard containing from 0.2 mg/ml to about1.5 mg/ml protein. A standard curve should be prepared each time the assay is performed. *For best results, the standard should be prepared in the same buffer as the sample.*
3. Pipet 5 µl of standards and samples into a clean, dry microtiter plate.
4. Add 25 µl of reagent A' or reagent A (see note from step 1) into each well.
5. Add 200 µl reagent B into each well. If microplate reader has a mixing function available, place plate in reader and let the plate mix for 5 seconds. If not, gently agitate the plate to mix the reagents. If bubbles form, pop them with a clean, dry pipet tip. Be careful to avoid cross-contamination of sample wells.
6. After 15 minutes, absorbances can be read at 750 nm. The absorbances willbe stable for about 1 hour. (See Troubleshooting Guide for recommendation on using a wavelength other than 750 nm.)

Section 6 Response of Various Proteins

As with any colorimetric assay, different proteins will elicit greater or lesser color formation. The following proteins have been assayed with the protein assay. As demonstrated by the graph, there is a slight variation in color development with different proteins.

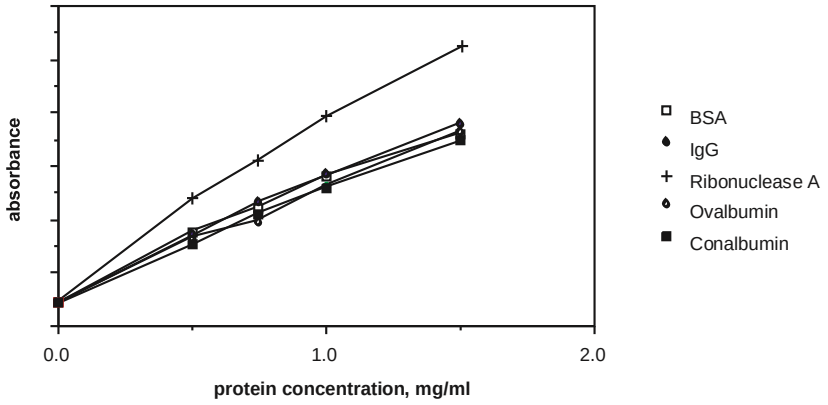

Section 7 Storage

Lyophilized preparations of Protein Standard I (bovine gamma globulin) and Protein Standard II (bovine serum albumin), if included, should be refrigerated upon arrival. These lyophilized preparations have a shelf life of one year at 4 °C. Rehydrated and stored at 4 °C, the protein solutions should be used within 60 days. Rehydrated and stored at -20 °C, the protein solutions should be used within 6 months.

REAGENT A, REAGENT B, and REAGENT S should be stored away from direct sunlight at room temperature (25-30 °C). (Reagents A and B may also be stored in the refrigerator.) All reagents are good for 6 months from date of purchase.

References

www.back.com/causes-mechanical-stenosis.html#

Adams, M. A., & Roughley, P. J. (2006). What is intervertebral disc degeneration, and what causes it? *Spine, 31*(18), 2151-2161. doi:10.1097/01.brs.0000231761.73859.2c

An, Yuehuei H., Martin,Kylie L.,. (2003). *Handbook of histology methods for bone and cartilage*. Totowa, NJ: Humana Press.

Ayroldi, E., Cannarile, L., Migliorati, G., Nocentini, G., Delfino, D. V., & Riccardi, C. (2012). *Mechanisms of the anti-inflammatory effects of glucocorticoids: Genomic and nongenomic interference with MAPK signaling pathways* doi:10.1096/fj.12-216382

Bergknut, N., Auriemma, E., Wijsman, S., Voorhout, G., Hagman, R., Lagerstedt, A. -., . . . Meij, B. P. (2011). Evaluation of intervertebral disk degeneration in chondrodystrophic and nonchondrodystrophic dogs by use of pfirrmann grading of images obtained with low-field magnetic resonance imaging. *American Journal of Veterinary Research, 72*(7), 893-898. doi:10.2460/ajvr.72.7.893

Bergknut, N., Grinwis, G., Pickee, E., Auriemma, E., Lagerstedt, A. -., Hagman, R., . . . Meij, B. P. (2011). *Reliability of macroscopic grading of intervertebral disk degeneration in dogs by use of the thompson system and comparison with low-field magnetic resonance imaging findings* doi:10.2460/ajvr.72.7.899

Bergknut, N., Meij, B. P., Hagman, R., De Nies, K. S., Rutges, J. P., Smolders, L. A., . . . Grinwis, G. C. M. (2013). *Intervertebral disc disease in dogs - part 1: A new histological*

grading scheme for classification of intervertebral disc degeneration in dogs doi:10.1016/j.tvjl.2012.05.027

Bergknut, N., Rutges, J. P. H. J., Kranenburg, H. -. C., Smolders, L. A., Hagman, R., Smidt, H. -., . . . Dhert, W. J. A. (2012). The dog as an animal model for intervertebral disc degeneration? *Spine, 37*(5), 351-358. doi:10.1097/BRS.0b013e31821e5665

Bergknut, N., Smolders, L. A., Grinwis, G. C. M., Hagman, R., Lagerstedt, A. -., Hazewinkel, H. A. W., . . . Meij, B. P. (2013). Intervertebral disc degeneration in the dog. part 1: Anatomy and physiology of the intervertebral disc and characteristics of intervertebral disc degeneration. *Veterinary Journal, 195*(3), 282-291. doi:10.1016/j.tvjl.2012.10.024

Bergknut, P. N. (2011). *Intervertebral disc degeneration in dogs.* [s.n.]).

Brisson, B. A. (2010). Intervertebral disc disease in dogs. *Veterinary Clinics of North America - Small Animal Practice, 40*(5), 829-858. doi:10.1016/j.cvsm.2010.06.001

Cappello, R., Bird, J. L. E., Pfeiffer, D., Bayliss, M. T., & Dudhia, J. (2006). Notochordal cell produce and assemble extracellular matrix in a distinct manner, which may be responsible for the maintenance of healthy nucleus pulposus. *Spine, 31*(8), 873-882. doi:10.1097/01.brs.0000209302.00820.fd

Cherrone, K. L., Dewey, C. W., Coastes, J. R., & Bergman, R. L. (2004). A retrospective comparison of cervical intervertebral disk disease in nonchondrodystrophic large dogs versus small dogs. *Journal of the American Animal Hospital Association, 40*(4), 316-320.

Erwin, W. M., Islam, D., Inman, R. D., Fehlings, M. G., & Tsui, F. W. L. (2011). Notochordal cells protect nucleus pulposus cells from degradation and apoptosis:

Implications for the mechanisms of intervertebral disc degeneration. *Arthritis Research and Therapy, 13*(6) doi:10.1186/ar3548

HANSEN, H. J. (1951). A pathologic-anatomical interpretation of disc degeneration in dogs. *Acta Orthopaedica Scandinavica, 20*(4), 280-293.

HANSEN, H. J. (1952). A pathologic-anatomical study on disc degeneration in dog, with special reference to the so-called enchondrosis intervertebralis. *Acta Orthopaedica Scandinavica.Supplementum, 11*, 1-117.

Hazewinkel, H. A. W., Meij, B. P., Bergknut, N., Tryfonidou, M. A., & Smolders, L. A. (2013). *Proefschrift luc smolders. new treatment strategies for canine intervertebral disc degeneration.* (). Retrieved from /z-wcorg/

Johnson, J. A., Da Costa, R. C., & Allen, M. J. (2010). Micromorphometry and cellular characteristics of the canine cervical intervertebral discs. *Journal of Veterinary Internal Medicine, 24*(6), 1343-1349. doi:10.1111/j.1939-1676.2010.0613.x

Kang, J. D., Georgescu, H. I., McIntyre-Larkin, L., Stefanovic-Racic, M., Donaldson III, W. F., & Evans, C. H. (1996). Herniated lumbar intervertebral discs spontaneously produce matrix metalloproteinases, nitric oxide, interleukin-6, and prostaglandin E2. *Spine, 21*(3), 271-277. doi:10.1097/00007632-199602010-00003

Kang, J. D., Stefanovic-Racic, M., McIntyre, L. A., Georgescu, H. I., & Evans, C. H. (1997). Toward a biochemical understanding of human intervertebral disc degeneration and herniation: Contributions of nitric oxide, interleukins, prostaglandin E2, and matrix metalloproteinases. *Spine, 22*(10), 1065-1073. doi:10.1097/00007632-199705150-00003

Kettler, A., & Wilke, H. -. (2006). Review of existing grading systems for cervical or lumbar disc and facet joint degeneration. *European Spine Journal, 15*(6), 705-718. doi:10.1007/s00586-005-0954-y

Kranenburg, H. J. C., Grinwis, G. C. M., Bergknut, N., Gahrmann, N., Voorhout, G., Hazewinkel, H. A. W., & Meij, B. P. (2013). Intervertebral disc disease in dogs - part 2: Comparison of clinical, magnetic resonance imaging, and histological findings in 74 surgically treated dogs. *Veterinary Journal, 195*(2), 164-171. doi:10.1016/j.tvjl.2012.06.001

Kumar, G. L. (2009). *Education guide : Immunohistochemical (IHC) staining methods*. Carpinteria, Calif: DAKO.

Levine, J. M., Levine, G. J., Johnson, S. I., Kerwin, S. C., Hettlich, B. F., & Fosgate, G. T. (2007a). Evaluation of the success of medical management for presumptive cervical intervertebral disk herniation in dogs. *Veterinary Surgery : VS, 36*(5), 492-499. doi:VSU00296 [pii]

Levine, J. M., Levine, G. J., Johnson, S. I., Kerwin, S. C., Hettlich, B. F., & Fosgate, G. T. (2007b). Evaluation of the success of medical management for presumptive thoracolumbar intervertebral disk herniation in dogs. *Veterinary Surgery : VS, 36*(5), 482-491. doi:VSU00295 [pii]

McGavin, M. Donald., Zachary,James F.,. (2007). *Pathologic basis of veterinary disease*. St.Louis: Elsevier Mosby.

Meij, B. P., & Bergknut, N. (2010). Degenerative lumbosacral stenosis in dogs. *Veterinary Clinics of North America - Small Animal Practice, 40*(5), 983-1009. doi:10.1016/j.cvsm.2010.05.006

Miyamoto, H., Doita, M., Nishida, K., Yamamoto, T., Sumi, M., & Kurosaka, M. (2006). Effects of cyclic mechanical stress on the production of inflammatory agents by nucleus pulposus and anulus fibrosus derived cells in vitro. *Spine, 31*(1), 4-9. doi:10.1097/01.brs.0000192682.87267.2a

O'Donnell, J. L., & O'Donnell, A. L. (1996). Prostaglandin E2 content in herniated lumbar disc disease. *Spine, 21*(14), 1653-5; discussion 1655-6.

Olby, N., Harris, T., Burr, J., Muñana, K., Sharp, N., & Keene, B. (2004). Recovery of pelvic limb function in dogs following acute intervertebral disc herniations. *Journal of Neurotrauma, 21*(1), 49-59.

Parker, H. G., VonHoldt, B. M., Quignon, P., Margulies, E. H., Shao, S., Mosher, D. S., . . . Ostrander, E. A. (2009). An expressed fgf4 retrogene is associated with breed-defining chondrodysplasia in domestic dogs. *Science, 325*(5943), 995-998. doi:10.1126/science.1173275

Pfirrmann, C. W. A., Metzdorf, A., Zanetti, M., Hodler, J., & Boos, N. (2001). Magnetic resonance classification of lumbar intervertebral disc degeneration. *Spine, 26*(17), 1873-1878. doi:10.1097/00007632-200109010-00011

Podichetty, V. K. (2007). The aging spine: The role of inflammatory mediators in intervertebral disc degeneration. *Cellular and Molecular Biology, 53*(5), 4-18. doi:10.1170/T814

Roberts, S., McCall, I. W., Menage, J., Haddaway, M. J., & Eisenstein, S. M. (1997). Does the thickness of the vertebral subchondral bone reflect the composition of the intervertebral disc? *European Spine Journal, 6*(6), 385-389. doi:10.1007/BF01834064

Royal, A. B., Chigerwe, M., Coates, J. R., Wiedmeyer, C. E., & Berent, L. M. (2009). Cytologic and histopathologic evaluation of extruded canine degenerate disks. *Veterinary Surgery, 38*(7), 798-802. doi:10.1111/j.1532-950X.2009.00570.x

Smolders, L. A., Bergknut, N., Grinwis, G. C. M., Hagman, R., Lagerstedt, A. -., Hazewinkel, H. A. W., . . . Meij, B. P. (2013). Intervertebral disc degeneration in the dog. part 2: Chondrodystrophic and non-chondrodystrophic breeds. *Veterinary Journal, 195*(3), 292-299. doi:10.1016/j.tvjl.2012.10.011

Thompson, J. P., Pearce, R. H., Schechter, M. T., Adams, M. E., Tsang, I. K. Y., & Bishop, P. B. (1990). Preliminary evaluation of a scheme for grading the gross morphology of the human intervertebral disc. *Spine, 15*(5), 411-415. doi:10.1097/00007632-199005000-00012

Tom Brock, P. D.Alzheimer's disease and arachidonic acid.

Urban, J. P. G., Smith, S., & Fairbank, J. C. T. (2004). Nutrition of the intervertebral disc. *Spine, 29*(23), 2700-2709. doi:10.1097/01.brs.0000146499.97948.52

van Dijk, B., Potier, E., Licht, R., Creemers, L., & Ito, K. (2014). The effect of a cyclooxygenase 2 inhibitor on early degenerated human nucleus pulposus explants. *Global Spine Journal, 4*(1), 33-40. doi:10.1055/s-0033-1359724 [doi]